Inhibition of Myofibroblast Contraction

by

Karolina A. Corin

S.B., Mechanical Engineering
S.B., Biology
Massachusetts Institute of Technology, 2003

Submitted to the Department of Mechanical Engineering in
Partial Fulfillment of the Requirements for the Degree of

Master of Science in Mechanical Engineering

at the

Massachusetts Institute of Technology

June 2005

Signature of Author..... .....
Department of Mechanical Engineering
May 19, 2005

Certified by..... .....
Ioannis V. Yannas
Professor of Polymer Science and Engineering
Thesis Supervisor

Accepted by..... .....
Lallit Anand
Professor of Mechanical Engineering
Chairman, Department Committee on Graduate Students

Inhibition of Myofibroblast Contraction

By

Karolina A. Corin

Submitted to the Department of Mechanical Engineering
On May 19, 2005 in Partial Fulfillment of the
Requirements for the Degree of
Master of Science in Mechanical Engineering

ABSTRACT

Although current medical procedures cannot restore complete function of a transected nerve, inserting both of its ends in a tube helps it regenerate. The regenerate is inferior to the uninjured nerve: it has a smaller diameter and poorer electrical conduction. Layers of contractile cells known as myofibroblasts have been observed around regenerated nerve portions. An inverse relationship between the layer thickness and the quality of the regenerate has also been observed. These findings suggest that the cells are exerting contractile forces which prevent the regenerating nerve from fully developing. Inhibiting this contraction should thus improve the quality of nerve regeneration.

Alpha smooth muscle actin (α-SMA) is a critical contractile protein. Its expression can be upregulated by the growth factor TGF-β1, and blocked by the pharmacological agent PP2. To investigate whether blocking SMA expression alone can inhibit myofibroblast contraction, NR6 wild type fibroblasts were seeded into short cylindrical collagen-GAG matrices, and administered either media alone, media with TGF-β1 (3ng/ml), or media with TGF-β1 and PP2 (10 μM). Non-seeded matrix samples were also prepared. The matrix diameters were measured every day for 12 days, after which the matrices were digested and the number of adhered cells were counted. The daily change in matrix diameter was calculated. The results showed that the cells contracted the matrices. TGF-β1 increased cell contractility, while PP2 inhibited it. Normalizing the Day 12 diameter change measurements to cell number and the original matrix diameter showed that TGF-β increased the strain generated by each cell ($1.85\text{x}10^{-6} \pm 2.79\text{x}10^{-7}$ relative to $6.43\text{x}10^{-7} \pm 3.40\text{x}10^{-7}$ for untreated cells), and that PP2 counteracted this effect ($6.33\text{x}10^{-7} \pm 1.09\text{x}10^{-6}$ strain/cell). Using the linear elastic constitutive relations, the average force exerted per cell was calculated for the untreated cells (3.36 ± 0.22 nN), TGF-β1 stimulated cells (9.69 ± 0.18 nN), and TGF-β + PP2 stimulated cells (3.31± 0.71 nN). The cell counts after Day 12 indicate that PP2 interferes with cell adhesion to the matrices. After 6 hours in culture, 21% of untreated cells, 25% percent of cells treated with TGF-β1, and 25% of cells treated with TGF-β1 and PP2 had adhered. By Day 12, only 12% of the seeded untreated cells, 14% of cells treated with TGF-β1, and 3.2% of cells treated with both TGF-β1 and PP2 remained adhered. This study thus indicates that PP2 inhibits cellular contraction, possibly by preventing cell-substrate adhesion.

Thesis Supervisor: Ioannis V. Yannas
Title: Professor of Polymer Science and Engineering

Acknowledgements

My thanks go to Professor Yannas for his advice, guidance, help, and support throughout this project. Thanks also go to Brendan for all of his help, training, and amazing advice – you really know it all. To Eric for … everything. It's been fun working with you. To Professor Spector and the rest of the FPL-ORL members for all of their input. To Jenny for listening. And most of all, to my parents.

Table of Contents

List of Figures

List of Tables

1.0 Introduction

1.1 The Peripheral Nervous System

1.11 Structure and Function

The peripheral nervous system (PNS) transmits electrical and chemical signals between the central nervous system (brain and spinal cord) and motor and sensory receptors, thereby regulating all movements and sensations (i.e. pressure, temperature) in the body. Neurons, specialized cells that can conduct electric impulses known as action potentials, allow this transmission to occur. The conductive neuron structure, the axon, is surrounded by an insulating tissue called the endoneurium. Thousands of these nerve fibers are encased in 2 more non-conducting tissue layers: the perineurium and the epineurium. Together they comprise a single nerve trunk.

Four main morphological structures enable neurons to conduct an action potential: the cell body, dendrites, axon, and axon terminal (Fig 1.11). The cell body houses the nucleus and other organelles essential for the cells' survival. Most protein and membrane production occurs here (Lodish *et al*, 2000). A long protrusion from the cell body is known as the axon. The axon, mainly composed of cytoplasm, the smooth endoplasmic reticulum, and microtubules, is the conducting section of the neuron. Action potentials originating from the axon hillock, the junction between the cell body and the axon, travel along the axon away from the cell body towards the axon terminal, the branched end of the axon. Each branch of the axon terminal is capable of making a synapse, or connection, with nearby cells. There are two types of synapses: a chemical synapse, and an electric synapse. When an action potential reaches a chemical synapse, signaling molecules known as neurotransmitters are released. When an electric synapse is reached, ions are released. Dendrites, protrusions from the cell body, receive these signals from the axon terminal of other neurons. The chemical or electrical signal detected by the dendrites is converted into electrical impulses and then transmitted to the cell body. The cell body is also capable of making a synapse with other neurons to receive signals.

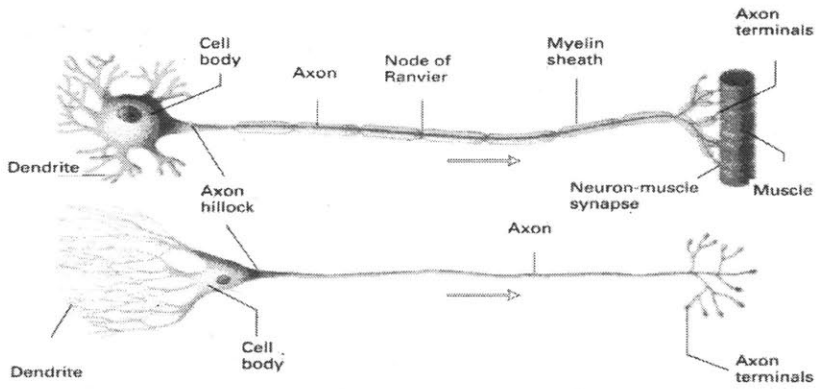

Figure 1.11: Neuron Morphology. (*Lodish, et al,* 2000) The cell body is the main body of the neuron. The axon conducts the action potential away from the cell body to the axon terminal, allowing the cell to communicate with other cells located near the terminal. Dendrites accept signals transmitted through the axon terminals. Some axons are surrounded by a myelin sheath produced by Schwann cells; gaps between various sections of the sheath are called nodes of Ranvier.

All axons are surrounded by Schwann cells, but only some are myelinated. Non myelinated axons are ensheathed by loosely wound Schwann cells. In this loose configuration, the Schwann cells maintain their cytoplasm. Myelinated axons are insulated in a thick layer of plasma membrane sheaths. These sheaths are produced when Schwann cells wrap around the axon. Tight wrapping of the Schwann cell plasma membrane around the axon, induced by the myelin protein P_o, (Lodish *et al*, 2000) forces most of the cytoplasm from the sheaths, creating a compact structure (Fig 1.12). Because each cell can only myelinate a 1-2 mm length (Harley, 2002), many Schwann cells are needed to mylinate the entire length of an axon. Gaps of about 2 μm, termed nodes of Ranvier, separate the myelin sheath of one Schwann cell from another. These nodes allow myelinated axons to transmit electrical signals more quickly than non-myelinated axons: the action potential travels progressively down a non-mylinated axon trunk, but is forced to jump from node to node in mylinated axons. Myelination only occurs in axons with a diameter greater than 0.7 μm (Yannas, 2001), where myelinated axons are typically 1-15 um in diameter. These axons typically target muscles or sensory organs. Non-myelinated axons are smaller, usually less than 1um, and comprise small pain nerves (Yannas, 2001). Both mylenated and non-myelinated axons are encased in a tubular basement membrane that completely covers the axons and the surrounding Schwann cells (including the nodes of Ranvier).

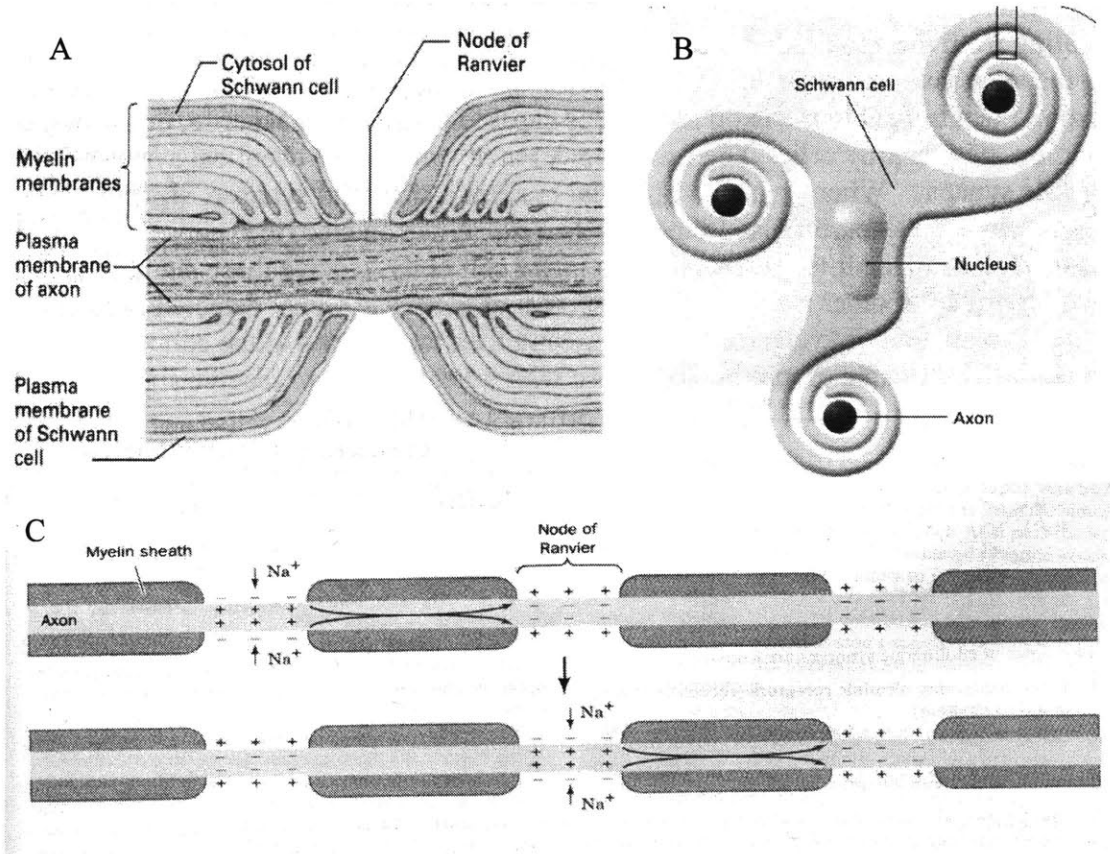

Figure 1.12: Schwann Cells and Mylinated Neurons. A) Axon section showing a closeup of the myelin layer. B) Schwann cell wrapped around three axons. C) Myelinated axon conducting an action potential; nodes of Ranvier are the gaps between myelin sheaths of different Schwann cells. (A and B from Lodish *et al* 2000, C from Voet and Voet, 1995)

Thousands of axons bundle together to form a fascicle. The fascicle is encased by the perineurium, a sheath of condensed, collagenous tissue. The perineurium creates an impermeable border between the inside endoneurium and, with multi-fascicular nerves, the outside epineurium. The endoneurium consists of blood vessels, fluids, and an extracellular matrix made of various proteins and cells, including collagens, proteoglycans, some integrin receptor proteins (e.g. fibronectin), fibroblasts, macrophages, and mast cells (Yannas, 2001). Axons are embedded and held fixed in this stroma by 2 sheaths of collagen fibrils. Those fibrils closer to the axon are interwoven, and sometime attach to the basement membrane. The outer sheath of fibrils is oriented longitudinally. The endoneurial blood vessels provide the stromal space with necessary molecules like water, ions, and plasma proteins. When a nerve consists of more than one fascicle, all of the fascicles are enclosed in a collagenous sheath called the epineurium. Collagen fibers of the epineurium are longitudinally oriented, and their average diameter decreases radially inward. The epineurium's main function is to protect the nerve from physical assault, like compressive forces (Yannas, 2001).

1.12 Activation of the System: The Action Potential

The action potential (Fig 1.13) is caused by a voltage change across the axon plasma membrane. The resting potential, or potential when the neuron is not conducting an electrical impulse, is about -60 mV (inside negative). Movement of ions across the axon membrane creates the voltage difference necessary for the propagation of an action potential. An action potential begins when the membrane is quickly depolarized, or when its potential is significantly increased due to an influx of positive ions (or exit of negative ions). This potential can be as high as 50 V (inside positive). Repolarization, the process in which the membrane potential is quickly returned to the resting potential, occurs quickly after depolarization. Ions causing the rapid depolarization and repolarization at one location on the axon membrane spread outward away from that site, thereby propagating the action potential down the axon.

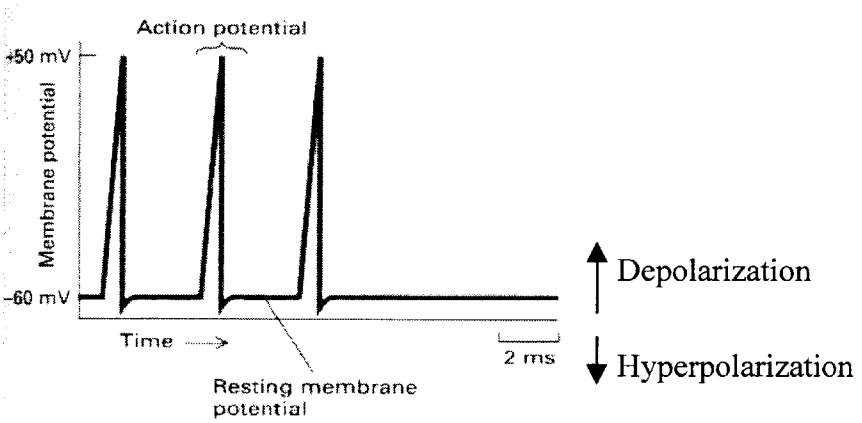

Figure 1.13: The Action Potential. (Lodish *et al*, 2001)

Potassium, sodium, and chloride ions are the three main "voltage-determining" ions. The concentration of K ions is higher inside the cell, while the concentration of Na and Cl ions is higher outside. These gradients are sustained by ATPases. Protein channels located in the axon membrane allow these ions to pass between the extracellular fluid and the intracellular fluid. There are two kinds of channels: resting ion channels, and voltage-gated ion channels. Voltage-gated ion channels only open in response to significant changes in the membrane potential. At the resting potential, these channels are closed. Resting ion channels are generally open. The axon membrane has a significant number of resting K channels – channels that are specific for K, and do not let other ions pass through. Potassium ions move through the channels down their concentration gradient. These channels, coupled with the presence of a few open Na and Cl channels, keep the membrane resting potential close to but less than (in magnitude) the potassium equilibrium potential. When the membrane is depolarized, voltage gated Na channels change conformation, allowing Na ions to pass through. The influx of Na ions into the cell down their concentration gradient leaves a net positive charge on the inside of the membrane, further depolarizing the region. Sodium ions stop migrating into the cell once the membrane potential is close to the sodium equilibrium potential, and the Na voltage-gated channels close. Spreading of Na ions inside the cell away from the site of depolarization induces depolarization in adjacent sections of the membrane, propagating the action potential. The channel-inactivating segment of voltage-gated channels prevents them from re-opening when the membrane has been depolarized, thus ensuring that the action potential can only travel in one direction. Once Na voltage-gated channels have begun to close, voltage-gated K channels open. Potassium ions exit the cell, repolarizing the membrane, and bringing it back to its resting potential. Because K voltage-gated channels remain open from the time of depolarizion until the membrane potential reaches a negative value, the membrane actually becomes hyperpolarized. This causes the membrane potential to briefly become more negative than the resting potential (Fig 1.14).

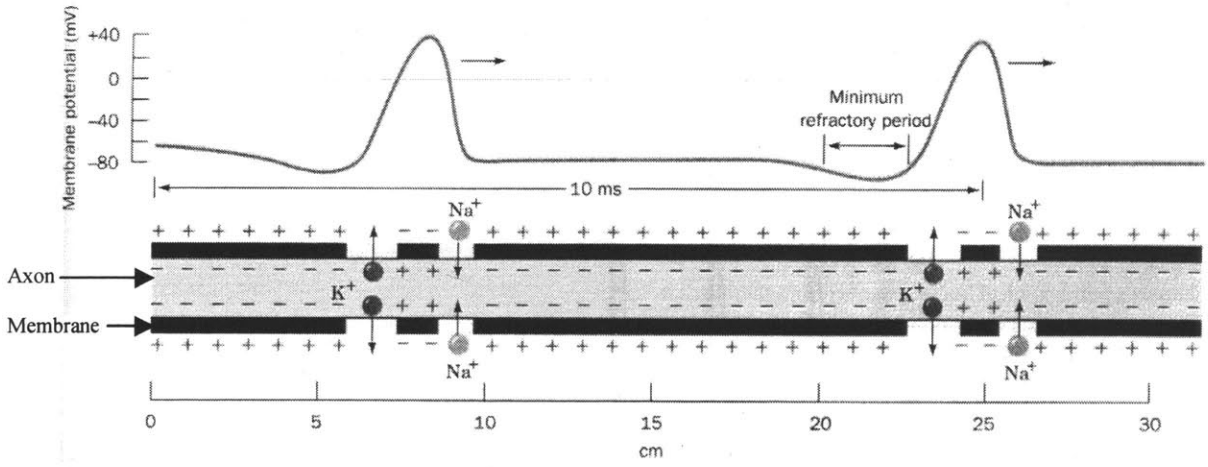

Figure 1.14: Axon membrane ion flux. Ion flux across the axon membrane induces the action potential that travels from the hillock to the terminal. (Voet and Voet, 1995)

1.2 Normal Injury Response of the PNS

Although peripheral nerves can be injured in a large variety of ways, two kinds of peripheral nerve injuries are commonly studied experimentally: crushing and transection. During crushing, a compressive force is applied to a section of a nerve. If mild, this force separates the axoplasm and the surrounding myelin sheath without injuring the basement membrane. During transection, the nerve trunk is completely severed, creating two nerve stumps. The nerve stump connected to the cell body is known as the proximal end, while the other stump is known as the distal end.

Nerves regenerate after suffering a crushing injury. Crushing displaces the axon and Schwann cell cytoplasm, and causes the myelin sheath to degenerate, creating a discontinuity in these structures at the point of compression. Because the nerve tube wall and the basement membrane remain intact, they are able to contain these tissues. Once the compressive force is released, the displaced tissues refill the gap space and reconnect, and the myelin sheath is regenerated. By ten weeks (or as little as four), the myelin sheath has completely regenerated, and nerve function is restored (Yannas 2001; Goodrum *et al*, 1995; Goodrum and Pentchev, 1997).

Nerves cannot always regenerate after they are transected. Following transection, both nerve stumps release an exudate containing macrophages, fibroblasts, and soluble regulators. Nerve fibers in the distal stump degenerate once they are separated from the cell body (Schmidt and Leach, 2003). Proteases dissolve their cytoskeletons and membranes, leaving columns of the surrounding Schwann cells. Collagen fibers accumulate around these columns. After 20-30 weeks, the Schwann cell columns shrink and occasionally fragment into pieces that are distributed into the intrafascicular space. Collagen fibers then fill the space created by the fragmented column. Eventually, collagen fibrils replace most of the space previously occupied by nerve fibers. Although the proximal stump does not degenerate, it does accumulate collagen fibrils. Cytokines in the surrounding fluid induce the axons in the proximal end to elongate. Most newly formed axons stem from the nodes of Ranvier (Schmidt and Leach, 2003). Reinnervation is achieved if the newly budding axons reach the distal stump, or reconnect with the previous target synapse. However, even if reinnervation occurs, the morphology of the repaired nerve is not normal. Fascicles originating in the proximal end split into many fascicles at the defect site. Each of these "daughter fascicles" contains axons, whose diameters are smaller than normal, encased in a perineurial sheath. The low conduction velocity of partially regenerated nerves has been attributed to this smaller diameter.

Transection can cause neuron death. The frequency of death increases as the distance between the transection site and the spinal cord decreases. Also, while motor neurons are likely to survive transection, sensory neurons are more sensitive. Up to 50% of sensory neurons die when they are severed (Harley, 2000).

1.3 Current Clinical Treatments

Sutures and nerve grafts are the two clinical treatments currently used to treat transected nerves (Schmidt and Leach, 2003).

Suturing involves surgically reconnecting the two ends of a transected nerve stump. This approach can only be used when the two nerve stumps are adjacent and less than 5 mm apart: suturing nerve ends that are farther apart induces tension that impedes nerve regeneration. Following suturing, about 25% of patients recover complete motor function, and 3% recover full sensory function (Harley, 2002).

Autologous nerve grafts are used to treat defects bigger than about 5 mm. A nerve graft procedure uses a functional nerve harvested from a donor site to connect the two ends of a transected nerve. The sural and saphenous nerves – two cutaneous nerves – are typically used as donor nerves (Schmidt and Leach, 2003) because of the available graft length (40 cm) and diameter (2-3 cm). Although up to 80% of patients recover function after grafting (Schmidt and Leach, 2003), the procedure has several disadvantages. The availability of donor sites is limited, and the patient must undergo several surgical procedures. Also, a secondary wound site must be created in order to harvest a graft, causing the patient to lose function at that site.

1.4 Current Therapeutic Research

Limitations and disadvantages of sutures and autologous grafts have prompted researchers to investigate other possible treatments. Therapies currently under investigation fall under three main categories: biomolecular therapies, cellular therapies, and guidance therapies (Schmidt and Leach, 2003).

Biomolecular therapy investigations mainly focus on determining which molecules promote regeneration, and developing methods to control delivery of these molecules to the wound site. Neurotrophins and other neurotrophic factors have been studied to determine which ones promote neuron survival and regeneration. These factors and their induced responses are listed in Table 1.41 (Schmidt et al, 2003). Various methods of delivery have been studied with varying degrees of success. Osmotic pumps and silicone reservoirs are potential vehicles for delivery, but they can fail and their non-degradable parts can cause inflammation or even infection. (Lewin et al, 1997; Schmidt and Leach, 2003; Maysinger and Morinville, 1997) Polymer matrices and microspheres have been effectively used to deliver molecules to nerve wounds, but their physical size limits the total amount of growth factors that they can contain, and hence release. This prompted investigations into potential viral and non-viral gene delivery methods. Viral vectors allow high expression of the gene that needs to be delivered, but they need to be tested for safety in clinical settings. Non-viral transfection techniques, like naked-DNA injection, gene guns, and lipoplexes are less risky than viral vectors, but they either have decreased gene expression, damage tissue, or are so poorly understood that they cannot be optimized. (Maysinger and Morinville, 1997; Schmidt and Leach, 2003)

Table 1.41: Neural Responses to Neurotrophic Factors

Neural Response Promoted	Neurotrophic Factors
Motor neuron survival	BDNF, NT-3, NT-4/5, CNTF, GDNF
Motor neuron outgrowth	BDNF, NT-3, NT-4/5, CNTF, GDNF
Sensory neuron survival	NGF, NT-4/5, GDNF
Sensory neuron outgrowth	NGF, BDNF, NT-3
Spinal cord regeneration	NGF, NT-3, CNTF, FGFs
Peripheral nerve regeneration	NGF, NT-3, NT-4/5, CNTF, GDNF, FGFs
Sensory nerve growth across the PNS-CNS transition zone	NGF, NT-3, GDNF, FGFs

Abbreviations: Brain-derived neurotrophic factor (BDNF), neurotrophin-3 (NT-3), neurotrophin-4/5 (NT-4/5), ciliary neurotrophic factor (CNTF), glial cell line-derived growth factor (GDNF), nerve growth factor (NGF), acidic and basic fibroblast growth factors (FGFs). The table was taken from Schmidt and Leach, 2003.

Cellular therapies try to use cells instead of molecules to aid in regeneration. Schwann cells have been shown to aid in axon elongation and functional regeneration (Schmidt and Leach, 2003; Yannas, 2001). Olfactory ensheathing cells (olfactory cells phenotypically similar to Schwann cells that assist axonal growth in the olfactory system by migrating with the axons) have also been shown to help. Macrophages have been extensively studied, but have yielded conflicting results. Some studies indicate that macrophages can help peripheral nerves regenerate, while other studies indicate that they inhibit regeneration (Schmidt and Leach, 2003). Altogether, more studies need to be conducted to determine the efficacy of any of these techniques.

Guidance strategies physically guide severed axons to their target. Allogenic and xenogenic grafts, tissue harvested from cadavers and animals, have been studied as possible substitutes for autologous grafts. Benefits include a larger supply source, and implantation surgeries that don't necessitate infliction of additional wounds in the patient. Potential problems include transmission of disease or invoking an immune response. Attempts have been made to remove or destroy immunogenic components of non-autologous tissues while preserving essential ECM components, but results so far have not yielded satisfactory results (Schmidt and Leach, 2003). Attention has thus been widely focused on using and/or finding synthetic materials that can aid in axon elongation and nerve regeneration. The possibility of using tubes to reconnect the ends of a severed nerve has probably been the most widely studied guidance therapy. Using tubes to connect the ends of a transected nerve has been shown to aid in its regeneration, at least as long as the gap does not exceed the critical axon elongation length[1] (Yannas, 2001). Much attention has thus been focused on optimizing this healing approach. Various tube materials and fillings have been studied, as well as the tube wall permeability and the pore orientation of the material comprising the tube. Although the optimal conditions have not been completely determined, some important discoveries

[1] The gap length at which the frequency of reinnervation for a given study population is 50%.

have been made. While several materials have been found that improve regeneration over the standard silicone tubes, collagen tubes appear to have yielded the best results: collagen tubes increased the critical axon elongation length the most. Nerves regenerated in collagen tubes also had smaller myofibroblast layers around them, bigger diameters, and better electrical conduction than nerves regenerated in silicone tubes. (Chamberlain *et al*, 1998; Chamberlain *et al*, 2000) Cell permeability of the tube wall, the presence of regulators (i.e. aFGF, bFGF), a controlled degradation rate, and axial orientation of the pore channels have also been shown to improve nerve regeneration. (Yannas, 2001; Harley *et al*, 2004; Yannas and Hill, 2004)

1.5 The Tissue Triad as a Model for Regeneration

1.51 Skin Organization and Regeneration

Skin is organized in three layers: the epithelia, the basement membrane, and the dermis (Fig 1.51). The epithelium is a thin, non-vascularized tissue layer that provides a protective barrier from environmental assault (i.e. microorganisms, skin moisture maintenance). The basement membrane is a non-vascular cell free layer that anchors the epidermis to the dermis via structures called rete ridges. The dermis is a thick vascularized layer located between the basement membrane and underlying muscles. It provides mechanical support and regulates the temperature of the organism. Capillaries loops within the rete ridges protruding from the dermis into the epidermis carry nutrients from the dermis to the two upper tissue layers. Appendages, like hair follicles, sweat glands, and oil-secretion glands are located in the dermis.

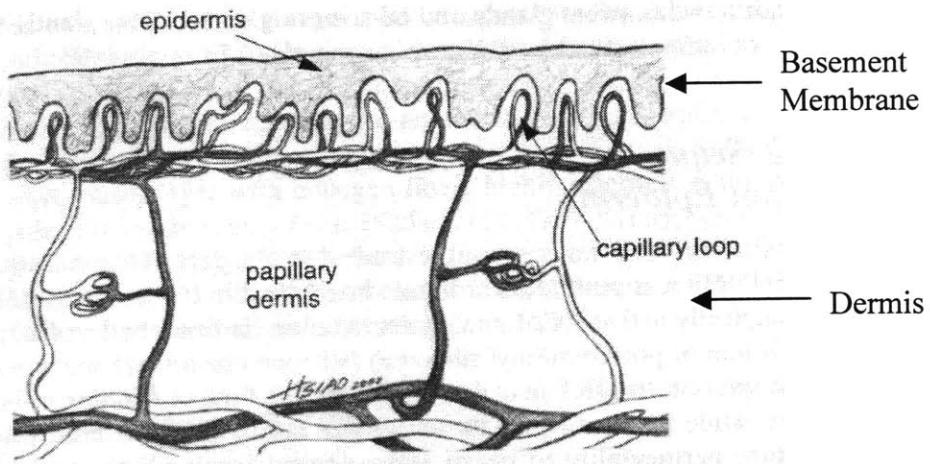

Figure 1.51: Organization of the Skin. (Yannas, 2001)

The epidermis and basement membrane regenerate spontaneously as long as the dermis is intact. The demis, however, does not regenerate. Instead, dermis-deep wounds mainly close by contraction, resulting in formation of scar tissue.

A dermis regeneration template (DRT) can be used to induce dermis regeneration. Fibroblasts migrate into the DRT pores after it has been placed in a dermis-free defect. Mechanical stresses and cytokines at the wound site induce fibroblasts to differentiate

into their contractile myofibroblast phenotype, but the DRT prevents closure of the wound by contraction: random cell alignment within the matrix pores prevents the cells from aligning and contracting along the same axis. The result is a regenerated dermis that is morphologically similar, though not identical, to the original tissue. The DRT does not help regenerate hair follicles, sweat glands, or other appendages located in the dermis. (Yannas, 2001)

1.52 Healing Response: Nerve-Skin Comparison

The tissues of the skin and peripheral nerve are similarly organized and behave comparably. Both have an epithelial layer (keratinocytes in skin and Schwann cells in nerves), basement membrane, and stroma (dermis in skin, endoneurial tissue in nerves). This tri-tissue configuration is known as the tissue triad (Figure 1.52). (Yannas, 2001) The epithelia and basement membranes in both organs are capable of regenerating, providing that the stroma remains intact. The stroma of both organs cannot regenerate on their own. Unaided, stromal wounds close and heal by contraction and scar formation. Administering a DRT to a dermis-free skin wound, however, induces regeneration by arresting contraction. Although skin tissues are planar and peripheral nerve tissues cylindrical, similarities between nerve and skin tissue organization and injury response indicate that arresting contraction during peripheral nerve repair may induce nerve regeneration or at least yield a higher-quality repaired nerve. The formation of a myofibroblast capsule around nerve regenerates indicates that this is the case. (Chamberlain, 2000) Nerves with thicker capsules exhibit poorer electrical conduction and smaller diameters than those with thinner layers. This indicates that the cells are contracting and exerting hoop stresses on the regenerate, thereby preventing complete healing. (Chamberlain *et al*, 1998; Spilker *et al*, 2000)

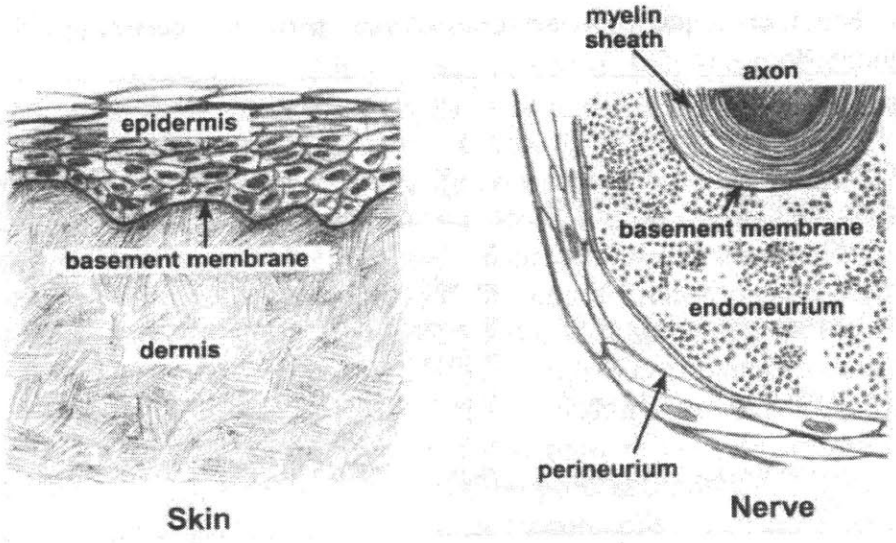

Figure1.52: The Tissue Triad in Skin and Nerves. (Yannas, 2001)

1.53 Role of Alpha Smooth Muscle Actin (αSMA) and Focal Adhesion Kinase (FAK) in Cell Contraction

FAK (focal adhesion kinase) is a protein involved in cell cytoskeleton organization and stress fiber formation. It has been implicated as an important component of many signaling transduction pathways (Aplin *et al*, 1998) including the one leading to expression of alpha smooth muscle actin in fibroblasts. (Desmouliere *et al*, 1992) Alpha smooth muscle actin (α-SMA) is a critical component of stress fibers, structures that allow cells to contract and generate forces. (Hinz *et al*, 2001; Hinz *et al*, 2003) Expression of the protein induces fibroblasts to differentiate into their contractile phenotype: myofibroblasts. (Scaffidi *et al*, 2001) Although the exact pathway from FAK to α-SMA expression is unknown[2], and most likely depends on cell type and stimulus, several key steps are known. The signaling pathway is probably initiated when a cell's integrins bind to an external substrate like the growth factor TGF-B or the ECM. This binding recruits FAK, as well as other proteins within the cell, to the focal adhesion site. At the site, FAK is activated by autophosphorylation. Once activated, it is able to bind to and activate other proteins downstream in the signaling pathway, like Grb2, Sos, and p130Cas. (Juliano, 2002; Aplin *et al*, 1998, Almeida *et al*, 2000) Eventually, the JNK (c-Jun N-terminal kinase) pathway is activated. (Tadashi *et al*, 1999; Aplin *et al*, 1998, Juliano, 2002; Almeida *et al*, 2000) In the final step of this kinase cascade, the terminal kinase c-Jun is phosphorylated. This enables it to enter the nucleus, bind to a transcription factor, and initiate gene expression. The exact protein number and order between FAK and the JNK pathway is unknown and potentially non-unique. (Tadashi *et al*, 1999; Cary and Guan, 1999) Figure 1.54 illustrates two possible pathways, beginning with integrin binding and ending with gene transcription.

[2] Research indicates that several pathways might exist. (Almeida *et al*, 2000)

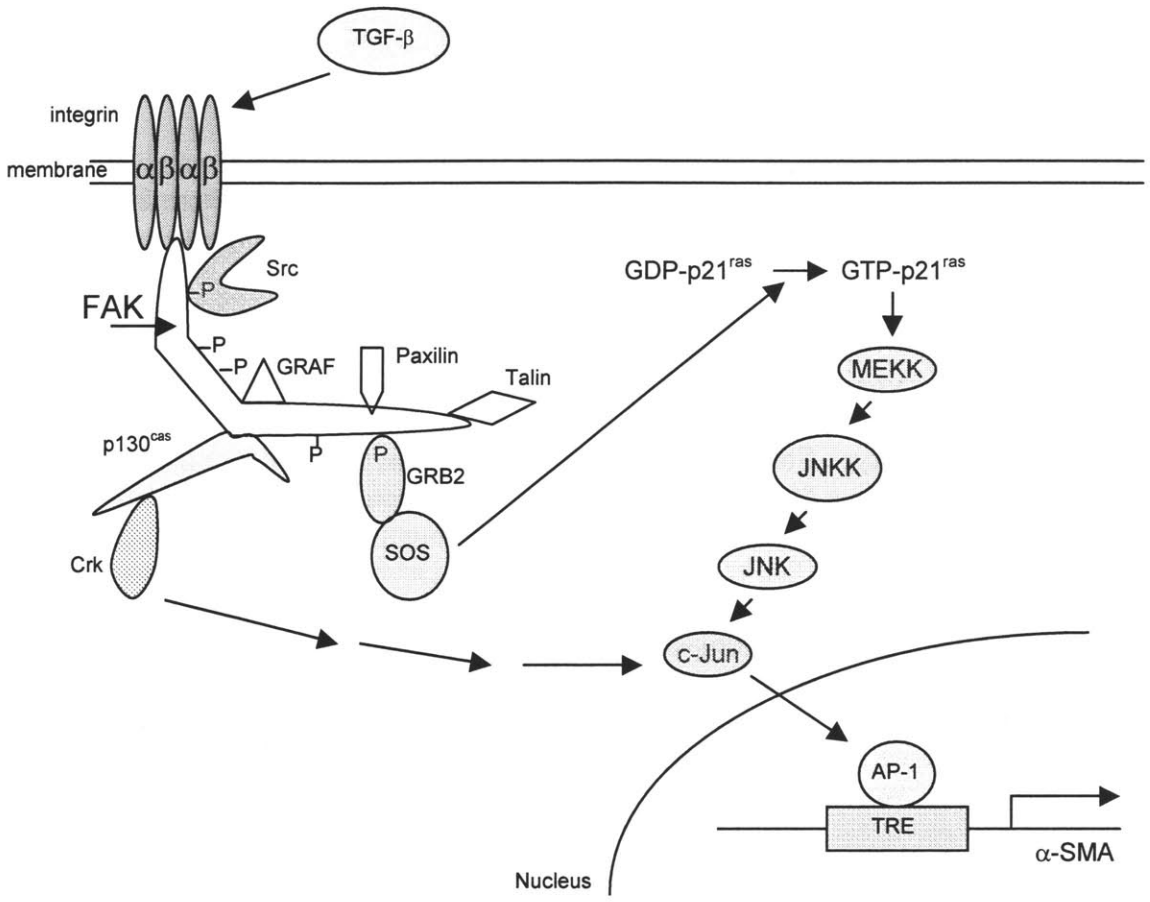

Figure 1.54: Two possible pathways leading to α-SMA expression. In one, FAK activation of p130Cas and Crk leads to JNK activation and α-SMA expression. In the other, Grb2 and Sos are the intermediaries. Adapted from Aplin *et al*, 1998; Tadashi *et al*, 1999, Johnson and Lapadat, 2002; Juliano, 2002; Li *et al*, 1996; Vaughan *et al*, 2000; Cary and Guan, 1999; Almeida *et al*, 2000; Girardin and Yaniv, 2001; Leuttich and Schmidt, 2003; Racine-Samson *et al*, 1997)

1.54 Inhibition of αSMA Expression and Cell Contractility

PP2 (4-amino-5-(4-chlorophenyl)-7-(*t*-butyl)pyrazolo[3,4-d]pyrimidine) is a pharmacological agent that prevents FAK phosphorylation, thereby blocking alpha smooth muscle actin expression and myofibroblast differentiation (Thannickal *et al*, 2003) Yoshizumi *et al* also demonstrated that PP2 blocks the JNK pathway. Because α-SMA induces differentiation of fibroblasts to myofibroblasts, thereby allowing them to contract and generate forces, and because PP2 inhibits myofibroblast differentiation and α-SMA expression, administering PP2 to fibroblasts should inhibit myofibroblast differentiation and contraction. If the nerve-skin comparison is accurate, then blocking cellular contraction around injured peripheral nerves should improve their healing response.

1.6 Methodology

1.61 Project Goal

This purpose of this project was to determine whether PP2 can be used to inhibit the contractile behavior of myofibroblasts. It is the first step in determining whether contraction-inhibiting pharmacological agents can be used to improve peripheral nerve regeneration.

1.62 Cell Type

NR6 wild type fibroblasts (NR6 wt) were used in the contraction experiments. NR6 wt's are a cell line derived from 17-19 day Swiss mouse embryos that have a human EGF receptor inserted in place of the natural mouse receptor. (Pruss & Herschman, 1977; Allen *et al*, 1999; Allen *et al*, 2002; Todaro and Green, 1963) Since transfection has been associated with decreased α-SMA expression (Okamoto-Inoue *et al*, 1990; Leavitt *et al*, 1985), primary fibroblasts would probably be the optimal cells to use: they should exhibit contractile behavior more similar to that of cells active in would healing. However, because NR6 wt's were readily available, are easier to culture, are fibroblastic, and have been shown to be contractile in collagen lattices (Allen *et al*, 1999; Allen, *et al* 2002), they were used instead.

1.63 Transforming Growth Factor-Beta1 (TGF-β)

TGF-β is a growth factor that induces fibroblasts to differentiate into myofibroblasts by upregulating α-SMA expression. (Dugina et al, 2001; Kunz-Schughart et al, 2003) It has been found in neural wound sites, and is associated with scar formation. Neutralization of TGF- β activity has been shown to improve nerve regeneration. (Davison *et al*, 1999; Rufer *et al*, 1994) It also induces cellular contraction of collagen-GAG matrices. (Zaleskas *et al*, 2001). Because of its demonstrated roles in contraction and in-vivo wound healing, TGF-β was chosen as the agonist to amplify the NR6 wt contractile response.

1.64 PP2

PP2 is a pharmacological agent that inhibits α-SMA expression by preventing FAK phosphorylation. Western blots indicate that PP2 can inhibit TGF-β-induced α-SMA expression. (Thannickal *et al*, 2003) It is thus hypothesized that TGF-β-induced cellular contraction is mediated through phosphorylation of FAK, and that PP2 can prevent this contractile response.

1.65 Assay

A free floating assay was used to evaluate the contractile responses of the cells. This type of assay is commonly used (Carlson and Longaker, 2004; Vickers, 2004), and offers benefits over other 2 or 3 dimensional assays. Alpha smooth muscle actin expression depends on whether cells are cultured on a two or three dimensional substrate. (Kunz-Schughart *et al,* 2003) It is thus preferable to use a 3D substrate as it is more representative of the wound environment. Cell force monitoring devices like those used by Freyman are difficult to use because cells need fresh media every 2-4 days: in these devices, cell feeding would likely cause matrix deformation or a disruption in the force measurement.

Collagen-GAG matrices were used as the substrates because they mimic the extracellular matrix naturally produced by cells. They have been widely used to study cell contraction, and have also been used to improve tissue regeneration in skin and nerve (Yannas, 2001; Freyman, 1996). Collagen is also an important receptor for long term force generation. (Sethi *et al*, 2002)

2.0 Materials and Methods

2.1 Collagen Scaffold Fabrication

All scaffolds were made by freeze-drying a collagen slurry, and then crosslinking the resulting matrix. The slurry was prepared by mixing type I microfibrillar bovine tendon collagen (Integra Life Sciences Corp., Plainsboro NJ) with 0.05M acetic acid, and blending the solution for 3 hours at 15,000 rpm at a constant temperature of 4° C. Chondroitin 6-sulfate (Sigma Aldrich Chemical Co., St. Louis MO) was added to the mixture halfway through the blending process. Once blending was complete, the slurry was degassed with a vacuum to remove large bubbles. Excess slurry that was not immediately used to make scaffolds was stored at 4° C. Slurry that had been stored for more than 2 weeks was re-blended and degassed again before use.

To fabricate the scaffolds, degassed slurry was transferred to aluminum molds with a square geometry. Bubbles found in the solution were pushed to the edge of the pan with a pipette tip. The molds were then placed in a freeze dryer, and the slurry was frozen to -40° C. In the final step, a vacuum was pulled (<300 Torr, 17 hours) to sublimate ice crystals, thus transforming the frozen slurry into a porous scaffold.

Dehydrothermal treatment (DHT) was used to crosslink the fabricated matrices: the matrices were placed in a vacuum oven for 24 hours (110° C). This process also served to sterilize the scaffolds.

The scaffolds were stored in a dessicator for long term storage. Detailed protocols on collagen matrix fabrication are in Appendix A.

2.2 Cell Culture

Cells were cultured in T75 (75 cm^2) flasks (VWR) in 17 ml of complete media (DMEM with 10% FBS and 1% Antiobiotic/Antimicotic, Invitrogen). They were kept in an incubator (37° C, 5% CO2, 95% relative humidity), and passaged when they were subconfluent.

The cells were obtained between passages 29 and 32 (P29-P32)[3]. They were grown up for 2 passages, and then frozen in DMSO cell freezing media (Invitrogen) at 2 million cells/ml (-80° C, liquid nitrogen). Prior to starting an experiment, one vial of cells was defrosted and split 1:4 for 2 passages, thus yielding 16 flasks for each experimental run. Cells used in the contraction assay were at P34. Complete cell culture, passaging, and freezing protocols are in Appendix B.

2.3 Matrix Seeding and Contraction Measurement

To measure cell-mediated contraction, the NR6 wt cells were seeded onto the fabricated matrices. Biopsy punches were used to cut matrix samples that were eight millimeters in diameter. (Figure 2.31) Each sample was placed in one well of a low-

[3] These cells were graciously given to our lab by Mike Berg and Jenny Lichter from the Rubner Lab at MIT. These cells originally came from the Lauffenburger lab at MIT.

adhesion 6-well plate. Three milliliters of phosphate buffered saline solution (PBS) were gently pipetted into each well to hydrate the matrices. After 30 minutes of hydration, the PBS was pipetted out of the wells. Blotting paper was then used to remove excess fluid in and around the scaffolds.

While the matrix samples were hydrating, a cell suspension with a concentration of about 32500 cells/μL (1.3 million cells per matrix) was prepared. After the matrices had been blotted, 20 uL of the suspension were pipetted onto one side of each matrix. After 10 minutes, the matrices were flipped over, and 20 uL of the cell suspension were pipetted onto the other side. The matrices were incubated for one hour to allow cells to adhere to them, and then 3 ml of media were added to each well. Six cell-seeded matrices had plain media added, 6 had media supplemented with TGF-β (3ng/ml), and 6 had media supplemented with TGF-β (3 ng/ml) and PP2 (10 μM). Additionally, 6 unseeded matrix samples were prepared. All samples were kept in the incubator for the duration of the experiment. The diameter of each matrix was measured each day for 12 days. The media was changed every two days. A detailed protocol is in Appendix C.

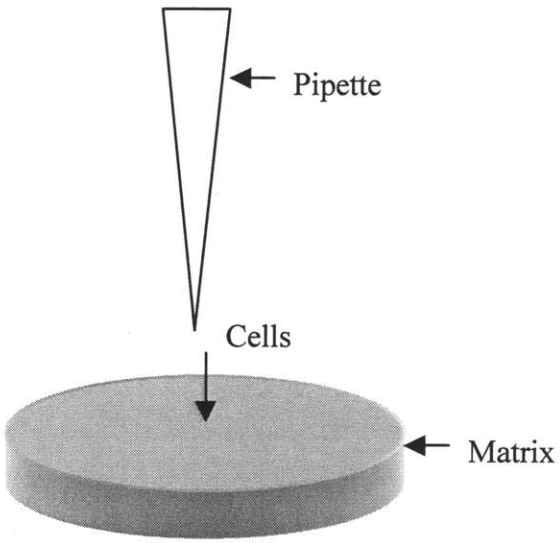

Figure 2.31: Matrix During Cell Seeding. Dermal biopsy punches were used to prepare matrix samples that were short cylinders (diameter >> height) with 8 mm diameters. Cells were seeded on the top surface of the matrices. After 10 minutes, the matrices were flipped over and the bottom side was seeded. Contraction of the diameter was measured over 12 days.

2.4 Matrix Degradation and Cell Counts

After 12 days in culture, the matrices were digested to count the number of adhered cells. Each sample was briefly washed in PBS to remove any non-adherent cells, and then placed in a pre-warmed dispase solution (2.525 mg/ml). After the matrices were completely digested, the cells were counted using a hemocytometer. Trypan blue was

used to distinguish between viable and non-viable cells. Four counts were performed for each sample. A detailed protocol is in Appendix D.

2.5 Statistical Analysis

The diameter decrease of each matrix sample was measured and graphed. From this data, cell-mediated contraction in the presence and absence of chemical regulators was calculated, and the resulting contractile forces exerted by the cells were estimated. A students t-test was used to determine statistical significance.

3.0 Results

3.1 Cell Viability

The number of adherent cells in the matrices decreased as the culture time increased. After 6 hours in culture, 21% of the untreated cells that had been seeded in the matrices had adhered (270,433 cells). Cells treated with TGF-β alone, and TGF-β in conjunction with PP2, each had about a 25% seeding efficiency (326,467 and 317,100 cells, respecitively). By Day 12, only 12% of the seeded untreated cells (154,667 cells), 14% of cells treated with TGF-β (182,933 cells), and 3.2% of cells treated with TGF-β and PP2 (41,800 cells) remained adhered to the matrices. All counted cells were viable. A dead cell count could not be determined: uptake of trypan blue by dead cells rendered them indistinguishable from the surrounding collagen debris. It is thus not possible to determine if cells died after entering and adhering to the matrices.

3.2 Matrix Contraction and Cell Force Generation

All of the samples decreased in diameter throughout the experiment, with the matrix + cells + TGF-β (TGF-β) samples contracting the most. Beginning on Day 3, there was statistical significance between the TGF-β samples and the rest of the samples ($p < 0.001$). While there was statistical significance between the matrix only (Matrix), and matrix + cells (Cells) samples ($p < 0.01$), the significance between either of these samples and the matrix + cells +TGF-β + PP2 (PP2) samples did not consistently remain significant throughout the experiment (sometimes $p < 0.001$, sometimes $p > 0.05$). All of the matrices decreased significantly by the last day of the experiment ($p < 0.001$): the Matrix sample decreased by 0.479 ± 0.251 mm in diameter, the Cells by 1.208 ± 0.292 mm, TGF-β by 2.938 ± 0.271 mm, and PP2 by 0.667 ± 0.204 mm. They also appeared to reach asymptotic values by Day 9. Figures 3.1 and 3.2 show the diameter and change in diameter for each sample over the course of the experiment.

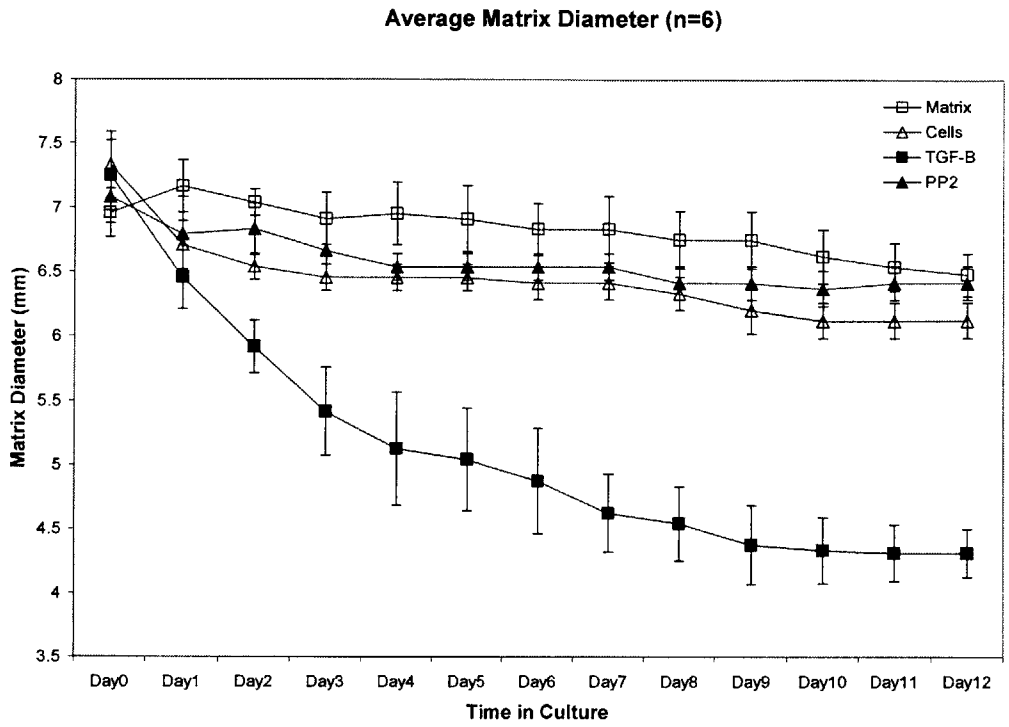

Figure 3.1: The average diameter for the unseeded matrices, and the treated and untreated seeded matrices over 12 days (n=6 for each sample). Error bars show the standard deviation.

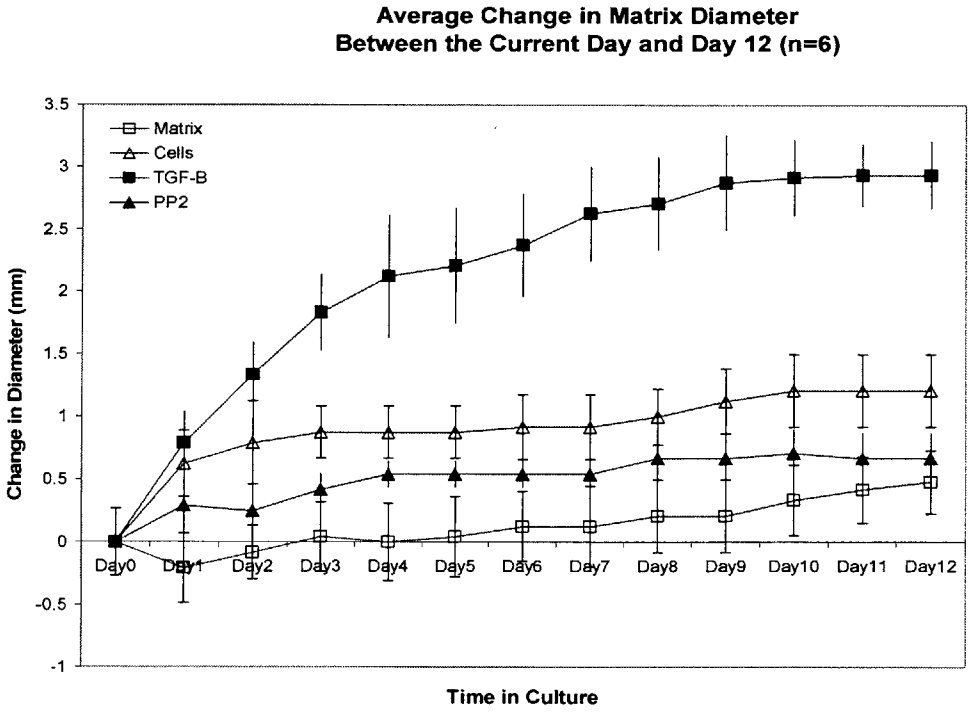

Figure 3.2: The average change in diameter for the unseeded matrices, and the treated and untreated seeded matrices over 12 days (n=6 for each sample). The change in diameter was calculated by subtracting the diameter read on any given day by that read on Day 0. Error bars show the standard deviation.

Subtracting the Matrix curve from the other curves yielded the contractile responses due solely to the cells (Figure 3.3). While these curves followed the same trends as the non-normalized curves, they began decreasing on Day 9. Although the decrease between Days 9 and 12 is not significant, it could indicate that the cells were either not pulling as hard, de-adhering from the matrix, migrating out of the matrix, or dying.

The Day 12 matrix-free responses were normalized to the Day 12 cell counts for each sample[4] and the original matrix diameters to show the average strain induced by each cell (Figure 3.4). TGF-β stimulated a three-fold increase in strain. PP2 counteracted TGF-β, bringing the level of contraction down to that observed in the non-induced state. There was no statistical significance between the Cell and PP2 samples, but there was a significant difference between the Cell and TGF-β samples ($p < 0.001$) and the PP2 and TGF-β samples ($p < 0.05$). The relatively high error seen in the PP2 data is due to lower cell counts. This data shows that TGF-β and PP2 affect the cells' ability to contract, and not just their ability to bind to and migrate within the matrices.

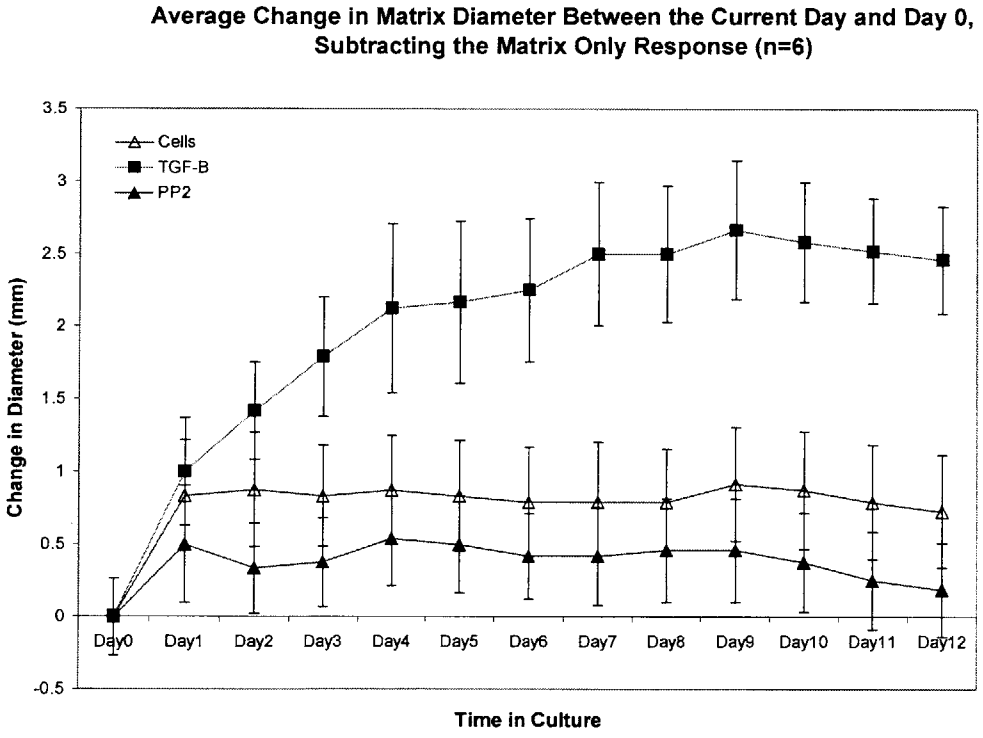

Figure 3.3: Cell-induced Contractile Response. These curves were obtained by subtracting the Matrix response from the three other curves in Figure 3.2. Error bars show the standard deviation.

[4] It was assumed that all cells counted, and hence present in the matrices, were contracting.

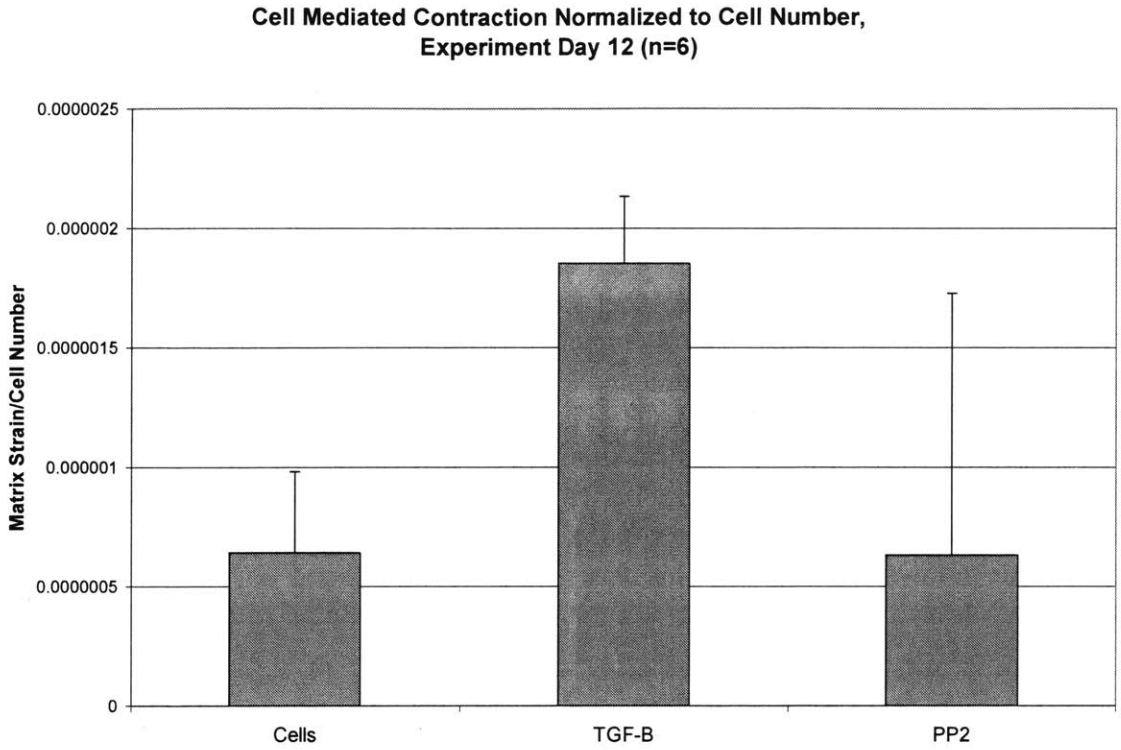

Figure 3.4: Average Cell-induced Strain. The Day 12 matrix-free data was normalized to the original matrix diameters and the cell numbers to determine the average strain per cell. All cells counted were assumed to be contracting. Error bars show the standard deviation.

The average force generated by each cell was estimated from the strain data using the isotropic linear elastic constitutive relations (Figure 3.5). The cells stimulated by TGF-β contracted with the greatest force (9.69 ± 0.182 nN), about three times that of non-stimulated cells (3.36 ± 0.222 nN) or those exposed to PP2 (3.31 ± 0.714 nN). The difference between the TGF-β stimulated cells and the other cells was significant ($p < 0.001$); there was no significant difference between the normal cells and those stimulated with PP2. The low error with the PP2 cells, relative to the high errors in the other graphs, comes from using a Taylor expansion to linearize nonlinear functions of random variables, as well as using linear transformations, to obtain the standard deviations.

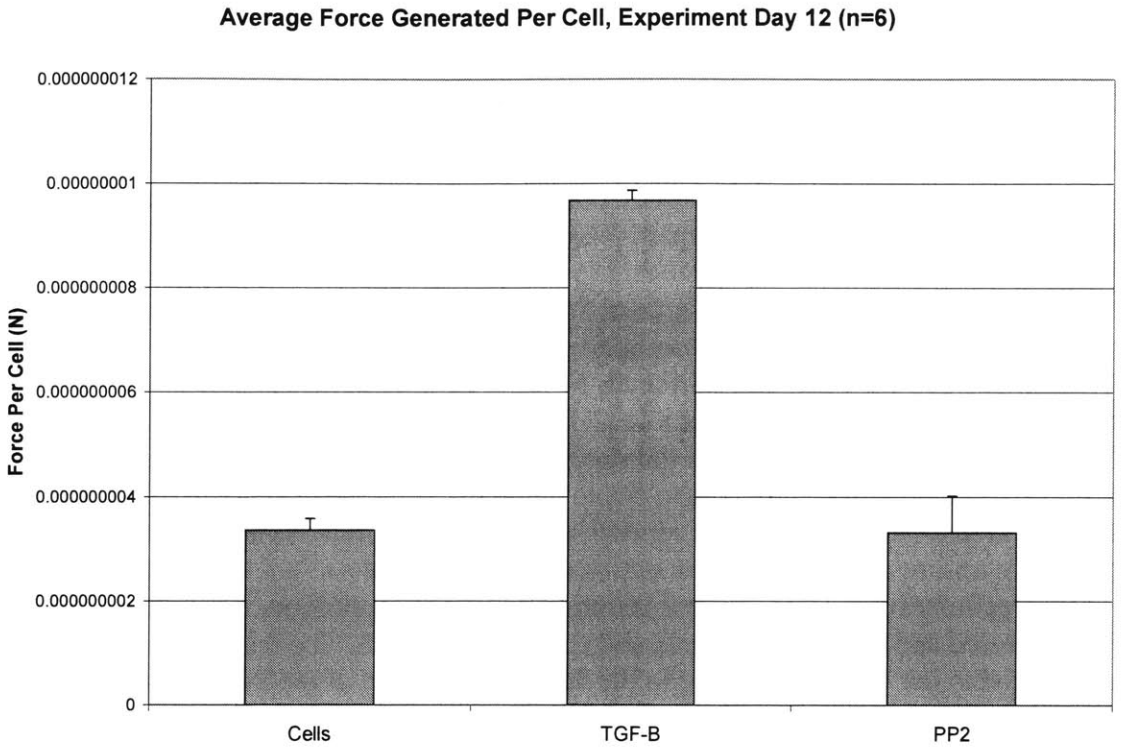

Figure 3.5: Average Force Generated By Each Cell. This force was estimated using the linear elastic constitutive relations, assuming that the axial and radial strains were approximately equal, and that there was no circumferential strain. Young's modulus was 208 Pa, and Poisson's ratio was taken as 0 (Harley *et al*, 2005). Error bars show the standard deviation.

4.0 Discussion

4.1 Data Analysis

The data shows that the NR6 cells are contractile in the collagen-GAG matrices, that TGF-β upregulates cellular contraction, and that PP2 counteracts this effect (Figures 3.2 and 3.3). While cellular contraction remains significant after Day 3, there is a slight decrease relative to the unseeded matrix samples after Day 9. Although the decrease between Days 9 and 12 is not significant ($p > 0.1$), it could indicate that the cells were pulling with less force, de-adhering from the matrix and releasing struts, migrating out of the matrix, or dying. Indeed, research indicates that free-floating matrices may not be conducive to cell proliferation. (Grinnell, 1994) Instead, cells prefer tensed substrates, and may even need them to generate large forces. (Grinnell, 2003; Arora *et al*, 1999) This decrease in contraction could thus be a result of using unstressed matrices. Although it could also reflect human errors in the diameter measurement, it is not likely: this type of error should introduce random variation, not a monotonic decrease over time.

To ensure that the observed strains were direct results of each stimulant's ability to affect cellular contraction and not cellular migration or adhesion, the matrix samples were digested and the number of adhered cells was counted. The matrix strains were then normalized to the cell counts. Due to the destructive nature of the assay, it was not possible to measure the number of adhered cells in each matrix for each day in culture. It was thus assumed that all of the matrices had a roughly equal seeding efficiency. The normalized data shows that TGF-β and PP2 affect the cells' ability to contract, and not just their ability to bind to and migrate within the matrices. TGF-β increases the deformation induced by each cell, and hence individual cell force generation. PP2 inhibits the TGF-β-induced matrix deformation and force generation. However, due to the relatively high error caused by the low cell counts, it is only possible to say that PP2 counteracts the effects of TGF-β. It is not possible to determine whether PP2 brings the level of force generation down to the level of the non-induced cells, below that level, or somewhere inbetween.

Although Figures 3.4 and 3.5 indicate that TGF-β and PP2 affect cell force generation, the cell counts indicate that they may also affect the number of cells migrating and adhering to the matrix. On Day 12, the matrices seeded with TGF-β-induced cells had slightly higher but similar cell counts as those seeded with untreated cells. Both of these cell counts were about 4 times as high (4.4 and 3.7 times as high, respectively) as those for the TGF-β and PP2-treated cells. The destructive nature of the assay precluded the possibility of determining whether each sample had the same number of cells initially seeded. It is thus possible that the lower PP2 count reflects a poor initial seeding efficiency. However, the initial seeding data obtained from separate matrix samples indicates that this is probably not the case, as all three cell-seeded samples had similar initial seeding efficiencies, and both the untreated cells and TGF-β-treated cells had comparable numbers of adhered cells at the end of the experiment. It thus seems likely that PP2 is either preventing cell proliferation, cell migration, or cell-matrix adhesion, or is causing apoptosis: FAK has been implicated as a protein involved in all four pathways. (Juliano, 2002; Cary and Guan, 1999) Use of PP2 in various in-vitro and in-vivo studies indicates that it is not toxic, and that apoptosis is probably not occuring

(Thannickal et al, 2003; Khadaroo et al, 2004; Lennmyr et al, 2004). However, this possibility cannot be discounted. Gene expression is influenced by the extracellular environment, and the effects of PP2 in a free-floating matrix have not been studied previously. Although the assay used could not quantify cell proliferation or migration, research indicates that PP2 may be amplifying the inhibitory effect of free-floating matrices on cell proliferation. (Grinnell, 1994) However, PP2 is probably preventing the cells from adhering to the matrices. FAK is an integral focal adhesion protein that is near the beginning of the α-SMA signaling pathway. Inhibition of α-SMA expression interferes with normal stress fiber formation, and inhibition of TGF-β (an inducer of α-SMA expression) prevents complete maturation of focal adhesions. (Dugina *et al*, 2001; Ronnov-Jessen and Petersen, 1996) Cells treated with PP2 are thus probably unable to synthesize the stress fibers necessary to attach to the matrices.

4.2 Error Analysis

Variations in the following four protocols are probably responsible for most of the experimental error: cell seeding, matrix diameter measurement, cell counting, and matrix blotting.

It is likely that the number of cells initially seeded onto each matrix varied from sample to sample. During seeding, the cell suspension was pipetted until it appeared to be evenly mixed. Equal volumes of the suspension were then pipetted onto each matrix. However, it is possible that the suspension wasn't homogenous at the time of seeding, or that the cells had settled between the time that the first and last matrix had been seeded. It is also probable that the suspensions were not distributed across the top surface in the same way on each matrix. Indeed, the suspension remained on the surface of some matrices until it was absorbed, while on others it spilled over the top. Most of the media that was on the matrix surfaces was absorbed, while most of the spill-over was not. As a result, this spill-over effectually reduced the number of cells in contact with the matrix, and hence the number of cells that were able to bind to and migrate into the matrices. The decreased seeding efficiencies that would result from any of these variations in protocol would have increased the calculated standard deviations.

Human error in the matrix diameter measurements accounts for much of the diameter variation from day to day. The measurements were made by placing the matrices over a sheet that had circles of various diameters on it. The diameter of the circle that best matched that of the matrix was recorded. Best estimates were made for those matrices that were not perfect circles. It was only possible to measure diameter changes in increments of 0.5 mm. Because the matrix diameters did not change significantly between consecutive days (with the exception of TGF-β), and because only increments of 0.5 mm were used, any diameter changes recorded for consecutive days is not significant. Indeed, it is not possible to determine whether any increases or decreases in matrix diameter for any 3 consecutive days is due to matrix contraction/expansion, or errors associated in manually determining the matrix diameter. Because of this, and because some matrices appeared to be contracting only along one axis (indicating either uneven cell seeding or a preferential direction of force generation), a non-destructive

computerized assay that could calculate the matrix surface area each day would be a better way to record matrix contraction.

The cell counting protocol may be a source of the error shown in Figure 3.4. To increase the accuracy of the total cell counts[5], all samples that had been similarly treated were digested together. The numbers obtained were then divided by the number of matrices to obtain an average cell count per matrix. As a result, the counts obtained reflected the total number of adhered cells for a given treatment, and not cell count of each individual matrix. However, it's possible that each matrix had a different number of attached cells, and that the variation in the contraction of each sample is due to the difference in cell number. It is thus possible that counting the number of cells in each matrix may have reduced the error.

The biggest source of error in the entire experiment may have come from blotting the matrices (Appendix C) because the amount of residual liquid would have affected two experimental parameters: the initial diameter and the number of cells infiltrating the matrix. During blotting, the edge of a thin strip of filter paper was placed next to a matrix. Once it had become saturated with PBS, a new piece was used to remove more PBS. This procedure was repeated for each matrix until it had been sufficiently blotted. Since it wasn't possible to measure the amount of residual PBS around the matrices prior to blotting, or the volume of PBS absorbed by the filter paper, each matrix was blotted until it appeared to have had the same amount of residual PBS as every other matrix. The matrices swell when they are hydrated, and contract when they are blotted. Thus, the matrices that had the most PBS removed through blotting would have had smaller initial diameters, which would have the effect of decreasing the statistical significance of the data. Also, since each matrix can only hold a given volume of media before becoming saturated, less cells would be able to absorb into poorly blotted matrices. Indeed, it is possible that the matrices in which the seeded cell suspension spilled over the top had more residual PBS than those in which the suspension remained confined to the surface. The poorer seeding efficiency resulting from insufficient blotting would also have decreased the statistical significance of the data.

4.3 Future Work

Although the initial data is promising, future studies need to be done to determine whether PP2 can be used to improve the nerve healing response. If possible, primary fibroblasts should be used since they would probably exhibit behavior more comparable to that of cells involved in would healing. All of the experiments need to be performed under more carefully controlled conditions to determine whether the low PP2 cell counts resulted from a low seeding efficiency, toxicity of PP2, or PP2-induced interference of cell-matrix adhesion. Stressed matrices may need to be used to aid in this determination. The experiments should also be done using differing concentrations of PP2 to find an optimal dose. Western blots analyzing α-SMA expression in each sample should be performed to confirm whether TGF-β and PP2 are acting according to the proposed model. If these experiments yield promising results, in-vivo experiments could be

[5] Very low cell concentrations yield highly variable cell counts. Digesting all similarly treated-matrix samples increased the number of cells present in each solution.

performed. These experiments will be the first true indicators of the efficacy of blocking cell contraction via an intracellular pathway to promote nerve regeneration.

5.0 Conclusion

It appears as though PP2 may not be the best agent to use to block cellular contraction. Although the data shows that PP2 does inhibit contractile forces generated by cells, it also indicates that PP2 may be causing cells to stop proliferating, de-adhere from the matrices, or possibly undergo apoptosis. The latter three effects are not desirable in wound healing. Cells need to be able to migrate to the wound site and adhere to agents that are present (i.e. other cells, existing extracellular matrix, clotting factors, biological scaffolds used for regenerative purposes, etc) in order to synthesize new tissue and repair the damaged tissue. If cells cannot localize to the wound site, then they cannot repair it. However, if they contract, they create scar tissue. It is thus necessary to find an agent that can inhibit contraction, but not cell-binding. It appears as though PP2 does both.

In contrast to this data, use of PP2 in vivo indicates that it may be used for healing purposes. (Khadaroo et al, 2004; Lennmyr et al, 2004) It is thus possible that experimental errors are masking the true effect of PP2. It is also possible that, while the in vitro response is valid, it is not indicative of an in vivo response. Many regulators and other stimuli are present in vivo, but not in vitro. Since FAK has been implicated as an upstream regulator of several intracellular pathways, and since the induced pathway may depend on a specific stimulus (i.e. stress, growth factors), response to PP2 will likely depend on cell type and environment. It is also possible that the cells used are not similar enough to in-vivo fibroblasts, or that the PP2 concentration used in the experiment was too high, and that an optimal dosage needs to be found. Thus, while more experiments need to be performed to determine the efficacy of PP2, it may also be prudent to investigate the possibility of using another inhibitor that acts more downstream in the α-SMA signaling pathway.

Appendix A. Collagen-Glycosaminoglycan Matrix Fabrication Protocols

A1. Collagen-Glycosaminoglycan (CG) Slurry Protocol (Harley, 2002)

Materials:

3.6 gm Type I microfibrillar bovine tendon collagen (Integra LifeSciences, Inc., Plainsboro, NJ)
2991.3ml distilled, deionized water
8.7 ml Glacial Acetic Acid
0.32 gm Chondroitin 6-sulfate (Sigma-Aldrich)

Procedure:

1. Turn on cooling system for blender (Ultra Turrax T18 Overhead blender, IKA Works, Inc., Wilmington, NC) and allow to cool to 4°C (Brinkman cooler model RC-2T, Brinkman Co., Westbury, NY).

2. Prepare 0.05 M acetic acid (HOAc) (pH 3.2) solution: add 8.7 ml HOAc (GlacialAcetic Acid, Mallinckrodt Chemical Co., Paris, KY) to 2991.3 ml of distilled, deionized water. This solution has a shelf life of approximately 1 week.

3. Blend 3.6 gm of microfibrillar bovine tendon collagen with 600 ml of 0.05 M acetic acid at 15,000 rpm (Setting: 3.25) for 90 minutes at 4°C.

4. Prepare chondroitin 6-sulfate solution: dissolve 0.32 gm chondroitin 6-sulfate (from shark cartilage: Cat. No. C-4384, Sigma-Aldrich Chemical Co., St. Louis, MO) in 120 ml 0.05 M acetic acid.

5. Calibrate peristaltic pump (Manostat Cassette Pump, Cat. No. 75-500-000, Manostat, New York, NY) to 120 ml per 15 minutes.

6. Add 120 ml of chondroitin 6-sulfate solution dropwise to the blending collagen dispersion over 15 minutes using the peristaltic pump, while maintaining the blender at 15,000 rpm (Setting: 3.25) and 4°C.

7. Blend slurry an additional 90 minutes at 15,000 rpm (Setting: 3.25) at 4°C.

8. Degas the slurry in a vacuum flask for 60+ minutes until bubbles are no longer present in the solution.

9. Store slurry in capped bottle at 4°C. Slurry will keep for up to four months.

10. If slurry has been stored for more than one week, reblend the slurry for fifteen minutes at 10,000 rpm (Setting: 2) at 4°C and degas again.

A2. Type I Collagen-GAG Matrix Fabrication Protocol (O'Brien *et al*, 2004)

Materials:

Type I collagen-glycosaminoglycan suspension (67.25ml/sheet)
5" x 5" stainless steel pan

Procedure:

1. Degas CG suspension in vacuum flask (Pressure: ~50mTorr).

2. Pipet 67.25ml of the CG suspension into the pan. Remove an air bubbles introduced into the pan using a 200µl pipette tip. Place the pan into the freeze-dryer.

3. Freeze CG suspension using a ramping protocol to produce uniform CG scaffolds:
   - Maintain freeze-drier chamber at 5°C for 5 minutes
   - Ramp the chamber temperature from 20°C to the final temperature of freezing (T_f = -40°C) at a rate of 0.9°C/min.
   - Maintain the chamber temperature at the final temperature of freezing for 60 minutes to finalize the freezing process.

4. Pull vacuum to commence the sublimation process. When the vacuum pressure in the chamber reaches below 300mTorr, raise the temperature of the chamber to 0°C. Allow the freeze-dryer to run for 17 hours at a temperature of 0°C and a pressure <300mTorr.

5. After 17 hours, raise the chamber temperature to 20°C. Wait for the chamber temperature to equilibrate to 20°C. Release the vacuum pressure and remove the scaffold from the freeze-drier.

6. Remove the CG scaffold from the pan with gloved hands. Place the scaffold into an aluminum foil packet and store in a dessicator.

A3. Dehydrothermal Crosslinking Protocol (adapted from Harley, 2002)

Procedure:

1. Place collagen material in aluminum foil packet. Leave packet open at top.

2. Place packet in vacuum oven (Isotemp Model 201, Fisher Scientific, Boston, MA).

3. Turn on vacuum. The vacuum oven should reach a final pressure of approximately -29.7 mmHg. Leave the matrix in the oven for 24 hours at 105°C.

4. At the end of the exposure period, turn off the vacuum and cent the chamber. Open the vacuum door and immediately seal the aluminum foil bags. The matrix is now crosslinked and considered sterile, so the matrix should only be handled under sterile conditions from now on.

5. Store the matrix in a dessicator. Crosslinked matrices can remain indefinitely in a dessicator prior to testing or use.

Appendix B: Cell Culture Protocols (adapted from Albers, 2004)

B1. Making Complete Media

Materials:

1 bottle DMEM (Dulbecco's Modified Eagle Medium, 12320032, Invitrogen, Carlsbad CA)
Fetal Bovine Serum (FBS, Hyclone, Lot ANM20369)
Antibiotic-Antimycotic (Penicillin/Streptomycin drugs, 15240062, Invitrogen)
5, 50 ml pipettes and pipette tips

1. Remove 55 ml DMEM from bottle and discard.
2. Add 50 ml FBS to DMEM bottle.
3. Add 5 ml drugs to DMEM bottle.
4. Mix.
5. Store at 4C.

Optional: put remaining FBS into 50 ml aliquots and freeze (avoids repeated thawing and freezing of FBS).

B2. Passaging Cells

Materials:

Pre-warmed complete media (DMEM with 10% FBS, 1% drugs)
Pre-warmed Dulbecco's Phosphate Buffered Saline Solution (PBS, Invitrogen)
Pre-warmed trypsin-EDTA (25300062, Invitrogen,)
Trypan blue (15250-01, Gibco, Grand Island, NY)

Equipment:

Hemacytometer, cleaned and washed (Bright-Line, Hausser Scientific, Horsham, PA)
Inverted microscope
Pipettes
10, 25, and 50 ml pipette tips
10, 200, 1000 μL pipettes and pipette tips
75 cm^2 tissue culture flasks (BD Falcon T-75, 353136)
Centrifuge (Labofuge 400, Heraeus)
50 ml Falcon tubes
1 ml Eppendorf tubes

Procedure:

1. Thaw and/or warm up complete media, PBS, trypsin-EDTA, in 37 C water bath (about 30 min before passaging).
2. Remove cells from incubator & place in hood
3. Remove media from culture flasks.
4. Wash cells in each flask with 5-6 ml PBS
    a. Shake gently
    b. Leave PBS on cells ~30 sec before pipetting PBS out of flask.
5. Pipette 4 ml trypsin in each flask and put cells in incubator 8 min.
6. While cells are in the incubator, prepare the hemocytometer.
    a. Clean hemocytometer and its cover slip with water and ethanol (EtOH).
    b. Check under the microscope for debris that can be mistaken for cells. If there is any, clean again. Otherwise, prepare the hemocytometer by adhering the coverslip to it with a drop of water on either side.
7. After 8 min, take the cells out of the incubator. Shake the flasks gently and check for cells floating in the trypsin (visible without microscope). Double check for non-adherent cells under the microscope. If the cells are still adherent, incubate them in trypsin a little longer. Otherwise put cells in hood and continue.
8. Deactivate the trypsin with 6 ml of media (volume can be varied depending on expected cell concentration).
9. Put the cells+media+trypsin in a 50 ml falcon tube.
10. Remove 100 uL of cells and transfer them to an eppendorf tube. Centrifuge the remainder of the cells at 2700 rpm for 5 min to pellet the cells.
11. While the cells are centrifuging, determine the cell the total cell number.

a. Add 100 uL trypan blue to the 100 uL of cells in the eppendorf tube.
b. Mix well.
c. Remove 10 uL and pipette it onto the hemocytometer.
d. Count the number of cells in a given number of squares (at least 5) using the counter.
e. Calculate the total cell number from the following formula:

   Total cell number = (# cells counted with hemocytometer)*(dilution factor in trypan blue)*10,000 * (# ml the 100 uL of cells were taken from)/(#squares counted on the hemocytometer)

f. Dispose of the trypan blue cells in a special waste container.
g. Wash off hemocytometer with water and ethanol.

12. After centrifuging, decant the media, being careful not to disturb the cell pellet.
13. Resuspend the cells in fresh media to the desired concentration.
14. Pipette the desired number of cells into culture flasks, and add media so that the final volume concentration is about 17 ml.
15. Put cells in incubator, changing media every 3-4 days if cells are not passaged. Passage the cells again when they subconfluent.
16. Clean everything, making sure to bleach any items that came in contact with cells.

Note: When using flasks that don't have vented caps, be sure that the cap is untwisted about a quarter or half turn while the cells are in the incubator.

B3. Defrosting Cells

Materials:

Pre-warmed complete media
Frozen cells
Trypan blue (15250-061, Gibco)

Equipment:

Water bath
Pipettes
1000 μL pipette tips
10, 25 ml pipette tips
Centrifuge (Labofuge 400, Heraeus)
Inverted Microscope
Hemacytometer (Bright-Line, Hausser)
50 ml Falcon tubes
1 ml Eppendorf tubes
Tissue culture flasks (BD Falcon T-75, 353136)

Procedure:

1. Warm up complete media in 37C water bath.
2. Remove desired number of vials w/ frozen cells from liquid nitrogen freezer (put on ice to transport anywhere).
3. Swirl each vial in 37C water bath until they just begin to defrost.
4. Add 1 ml complete media to each vial and let the cells thaw completely. Once thawed, gently pipette the cells up and down to evenly distribute them in the media.
5. Transfer cells from the vials into 50 ml Falcon tubes (either combine all the cells or use different tubes for different vials, depending on the experiment) and add complete media until the tube is mostly full.
6. Spin the tube(s) down at 2700 rpm for 5 min to pellet the cells.
7. Remove old media and resuspend the cells in 10 ml fresh media (volume can be changed depending on desired and expected cell concentrations)
8. Remove 100 uL resuspended cells and transfer to an eppendorf tube.
9. Add 100 uL trypan blue and mix thoroughly.
10. Remove 10 uL of the mixture and transfer to a prepared hemocytometer. Count the cells and determine the total cell number.
11. Add the desired number of cells to cell culture flasks, and add enough media to cover the area of the flask on which cells will adhere (17 ml for 75 cm flask).
12. Put cells in incubator, and passage them when they become subconfluent.

B4. Freezing Cells

Materials:

Pre-warmed complete media (DMEM with 10% FBS, 1% drugs)
Pre-warmed PBS (Invitrogen)
Pre-warmed trypsin-EDTA (25300062, Invitrogen)
Trypan blue (15250-061, Gibco)
DMSO Cell Freezing Media (11101-011, Invitrogen)

Equipment:

Hemacytometer (Bright-Line, Hausser Scientific)
Inverted microscope
Pipette-man
10, 25, and 50 ml pipette tips
10, 200, 1000 µL Pipettes and pipette tips
75 cm^2 tissue culture flasks (VWR, 29181-105)
Centrifuge (Labofuge 400, Heraeus)
50 ml Falcon tubes
1 ml Eppendorf tubes
2ml cryovials

Procedure:

1. Follow steps 1-12 of the Passaging protocol (Appendix B2).
2. Resuspend the cell pellet in DMSO. Add DMSO until the final cell concentration is 1-2 million cells/ml.
3. Make 1 ml aliquots of the cell suspension in cryovials.
4. Freeze in liquid nitrogen immediately.

Appendix C: Matrix Seeding and Contraction Measurement (adapted from Vickers *et al*, 2004)

C1. Protocol

Materials:

8 mm dermal biopsy punches (Lot 04129, Miltex, York, PA)
Low adhesion 6-well plates (3471, Corning, Corning, NY)
NR6 wt cells at passage less than 50
PP2 (529573, Calbiochem, San Diego, CA)
TGF-β1 (T-7039, Sigma, St. Louis, MO)
Complete media
Blotting paper (cut into 5mm x 20 mm strips)
One sheet of fabricated collagen-GAG matrix
PBS (Invitrogen)
Matrix measurement template

Equipment:

50 ml Falcon tubes
Forceps
5, 10, 25 ml pipettes and pipette tips
10, 20, 1000 μL pipettes and pipette tips
Water bath
Centrifuge

Procedure:

1. Pre-warm the complete media and PBS in the water bath
2. Using the biopsy punches, cut out matrix samples from the collagen-GAG sheet. Push down on the matrix when using the punch – do not twist. Use a new punch after every six cuts. Put each cut matrix sample in one well of a low adhesion 6-well plate. Prepare 4 plates (24 matrix samples).
3. Slowly and gently pipette PBS onto the matrices to hydrate them. Add enough PBS to cover the matrices.
4. Let the matrices sit in the PBS for 30 minutes. Then pipette the PBS out of the wells, making sure not to disturb the matrices with the pipette tip.
5. Remove residual PBS surrounding the matrices with blotting paper. Place the edge of the blotting paper next to the matrix to allow it to soak up PBS. After it has become saturated, replace it with another strip of blotting paper. Repeat until the matrix no longer sits in a pool of media and is not fully saturated with liquid. Do not place the paper directly onto the matrix – they will stick together.

6. Prepare a cell suspension of about 1.3 million cells/40 μL using the cell passaging protocol (Appendix B2). The total suspension volume should be 720 μL (40 μL for each matrix that will be seeded with cells).
7. Pipette 20 μL of the suspension onto the top surface of 18 blotted matrices. Pipette 20 μL of complete media onto the other six samples.
8. After 10 minutes, flip the matrices over with forceps. Avoid deforming the matrices.
9. Pipette an addition 20 μL of the cell suspension or complete media onto the matrices.
10. Put the samples in the incubator for 1 hour to allow the cells to enter and adhere to the matrix.
11. While the samples are incubating, prepare the following solutions: 36 ml of complete media, 18 ml of complete media with 3 ng/ml of TGF-β, and 18 ml of complete media with 3 ng/ml of TGF-β and 10 μM PP2. Keep the media solution warm until they are ready to be used.
12. After the 1 hour incubation, remove the samples from the incubator and add the media solution. In the non-seeded plate and in one plate of cell-seeded matrices add 3 ml of complete media to each well. These are the Matrix only and Cells only samples. Add 3 ml of complete media with 3 ng/ml of TGF-β to each well of the second plate of cell-seeded matrices. These are the TGF- β samples. Add 3ml of complete media with 3 ng/ml of TGF-β and 10 μM PP2 to each well of the third plate of cell-seeded matrices. These are the PP2 samples.
13. Record the diameter of each matrix using the template.
14. Place the matrices in the incubator.
15. Record the matrix diameter every day.
16. Change the media every 2 days.
17. After 12 days in culture, digest the matrices and count the number of adhered cells.
18. To obtain an initial seeding efficiency count, repeat steps 1-14. After 6 hours in culture digest the matrices and perform a cell count.

C2. Matrix Measurement Template

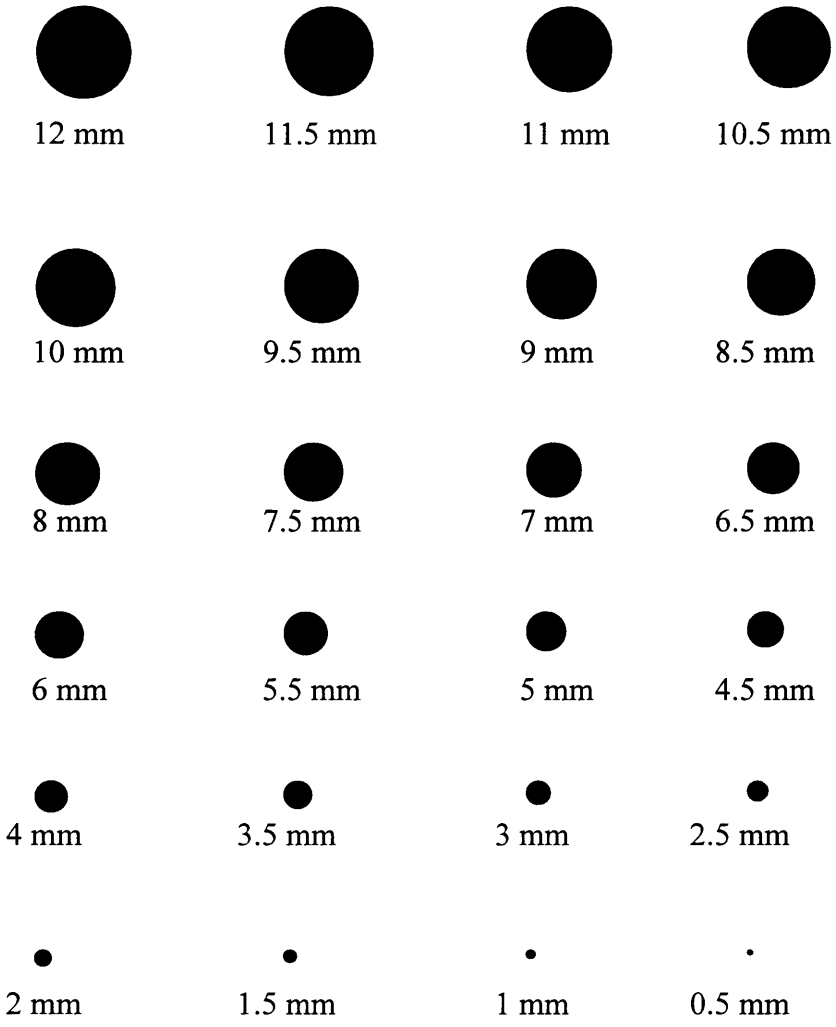

Appendix D: Matrix Degradation and Cell Counting Protocol (adapted from Freyman, 1996)

Materials:

Dispase (Gibco)
Pre-warmed Dulbecco's Phosphate Buffered Saline Solution (Invitrogen)
Trypan Blue (Gibco)

Equipment:

Water Bath
Forceps
Hemacytometer (Bright-Line, Hausser Scientific)
Inverted microscope
Scale
Eppendorf Tubes
5, 10 ml pipettes and pipetters
20, 200 μL pipettes and pipette tips

Procedure:

1) Prepare a PBS wash solution by pipetting 12 ml PBS into a 15 ml tube.
2) Make a dispase solution of 2.4 U/mL dispase in 12 ml PBS for each matrix sample.
3) Using forceps, gently immerse each matrix in the PBS wash.
4) Transfer the matrices to the dispase solution. Place each similarly treated matrix in the same dispase solution (each tube should have 6 matrices in 12 ml of dispase solution).
5) Incubate at 37° C until the matrices have been completely digested.
6) Perform 4 separate cell counts on each digest using the same counting procedure in the Cell Passaging Protocol (Appendix B2, Step 11).
7) From the counts, determine the average number of cells in each matrix.

References

1. Albers A., (2004) MS. Thesis, Massachusetts Institute of Technology, Cambridge, MA.
2. Allen F.D., Asnes C.F., Chang P., Elson E.L., Lauffenburger D.A., Wells A., (2002). Epidermal growth factor induces acute matrix contraction and subsequent calpain-modulated relaxation. *Wound Repair Regen.* 10(1): 67-76.
3. Allen F.D., Asnes C.F., Wells A., Elson E.L., Lauffenburger D.A., (1999). Epidermal Growth Factor Mediated Contractile Force in NR6 Fibroblast Cells Grown in a Collagen Lattice. Bioengineering Conference, June 16-20, Big Sky Montana, Paper number a0082714.
4. Almeida E.A.C., Ilic D., Han Q., Hauck C.R., Jin F., Kawakatsu H., Schlaepfer D.D., Damsky C.H., (2000). Matrix Survival Signaling: From Fibronectin via Focal Adhesion Kinase to c-Jun NH_2-terminal Kinase. *J Cell Biol.* 149(3): 741-54.
5. Aplin A.E., Howe A., Alahari S.K., Juliano R.L., (1998). Signal Transduction and Signal Modulation by Cell Adhesion Receptors: The Role of Integrins, Cadherins, Immunoglobulin-Cell Adhesion Molecules, and Selectins. *Pharmacalogical Reviews.* 50(2): 197-263.
6. Arora P.D., Narani N., McCulloch C.A., (1999). The Compliance of Collagen Gels Regulates Transforming Growth Factor-Beta Induction of Alpha-Smooth Muscle Actin in Fibroblasts. *Am J Pathol.* 154(3): 871-82.
7. Carlson, M.A., Longaker M.T., (2004). The fibroblast-populated collagen matrix as a model of wound healing: a review of the evidence. *Wound Repair Regen,* 12(2): 134-47.
8. Cary L.A., Guan J.-L., (1999). Focal Adhesion Kinase in Integrin-Mediated Signaling. *Front Biosci.* 4:D102-13. Review.
9. Chamberlain L.J., Yannas I.V., Arrizabalaga A., Hsu H.-P., Norregaard T.V., Spector M., (1998). Early Peripheral Nerve Healing in Collagen and Silicone Tube Implants: Myofibroblasts and the Cellular Response. *Biomaterials.* 19(15): 1393-403.
10. Chamberlain L.J., Yannas I.V., Hsu H.P., Spector M., (2000). Connective Tissue Response to Tubular Implants for Peripheral Nerve Regeneration: the Role of Myofibroblasts. *J. Comp. Neurol.* 417(4):415-30.
11. Davison S.P., McCaffrey T.V., Porter M.N., Manders E., (1999). Improved Nerve Regeneration with Neutralization of Transforming Growth Factor-beta1. *Laryngoscope* 109(4): 631-5.
12. Desmouliere A., Rubbia-Brandt L., Abdiu A., Walz T., Maceira-Coelho A., Gabbiani G., (1992). α-Smooth Muscle Actin is Expressed in a Subpopulation of Cultured and Cloned Fibroblasts and is Modulated by γ-Interferon. *Exp Cell Res.* 201(1): 64-73.
13. Dugina V., Fontao L., Chaponnier C., Vasiliev J., Gabbiani G., (2001). Focal Adhesion Features During Myofibroblast Differentiation Are Controlled by Intracellular and Extracellular Factors. *J Cell Sci.* 114(Pt 18): 3285-96.

14. Freyman T.M. (1996). Development of an In Vitro Model of Contraction by Fibroblasts. PhD Thesis, Massachusetts Institute of Technology, Cambridge, MA.
15. Girardin S.E., Yaniv M., (2001). A Direct Interaction Between JNK1 and CrkII is Critical for Rac1-induced JNK Activation. *The EMBO Journal.* 20(13): 3437-46.
16. Goodrum J.F., Bouldin T.W., Zhang S.H., Maeda N., Popko B., (1995). Nerve Regeneration and Cholesterol Reutilization Occur in the Absence of Apolipoproteins E and A-1 in Mice. *J. Neurochem.* 64, 408-416.
17. Goodrum J.F., Pentchev P.G., (1997). Cholesterol reutilization during myelination of regenerating PNS axons is impaired in Niemann-Pick disease type C mice. *J. Neurosci Res.* 1:49(3):389-92.
18. Grinnell, F., (2003) Fibroblast biology in three-dimensional collagen matrices. *Trends Cell Biol,.* 13(5): 264-9.
19. Grinnell, F., (1994). Fibroblasts, myofibroblasts, and wound contraction. *J Cell Biol*, 124(4): 401-4.
20. Harley B.A. (2002). Peripheral Nerve Regeneration Through Collagen Devices with Different In Vivo Degradation Characteristics. M. S. Thesis, Massachusetts Institute of Technology, Cambridge, MA.
21. Harley B.A., Spilker M.H., Wu J.W., Asano K., Hsu H.–P., Spector M., Yannas I.V., (2004). Optimal Degradation Rate for Collagen Chambers Used for Regeneration of Peripheral Nerves over Long Gaps. *Cells Tissues Organs.* 176: 153-65.
22. Harley B. A., Yannas I.V., and Gibson L.J., (2005, in preparation for submission). Mechanical Characterization of a Homologous Series of Equiaxed Collagen-GAG Scaffolds.
23. Hinz B., Celetta G., Tomasek J.J., Gabbiani G., Chapponier C., (2001). Alpha-Smooth Muscle Actin Expression Upregulates Fibroblast Contractile Activity. *Mol Biol Cell.* 12(9): 2730-41.
24. Hinz B., Dugina V., Ballestrem C., Wehrle-Haller B., Chapponier C., (2003). α-Smooth Muscle Actin is Crucial for Focal Adhesion Maturation in Myofibroblasts. *Mol Biol Cell.* 14(6): 2508-19.
25. Johnson G., Lapadat R., (2002). Mitogen-Activated Protein Kinase Pathways Mediated by ERK, JNK, and p38 Protein Kinases. *Science.* 298: 1911-12.
26. Juliano R.L., (2002). Signal Transduction by Cell Adhesion Receptors and the Cytoskeleton: Functions of Integrins, Cadherins, Selectins, and Immunoglobulin-Superfamily Members. *Annu. Rev. Pharmacol. Toxicol.* 42: 283-323.
27. Khadaroo R.G., He R., Parodo J., Powers K.A., Marshall J.C., Kapus A., Rotstein O.D., (2004). The role of the Src family of tyrosine kinases after oxidant-induced lung injury in vivo. *Surgery* 136(2): 483-8.
28. Kunz-Schughart L.A., Wenninger S., Neumeier T., Seidl P., Kneuchel R., (2003). Three-dimensional Tissue Structure Affects Sensitivity of Fibroblasts to TGF-beta 1. *Am J Physiol Cell Physiol.* 284(1): C209-19.
29. Leavitt J, Gunning P, Kedes L, Jariwalla R. (1985). Smooth muscle alpha-action is a transformation-sensitive marker for mouse NIH 3T3 and Rat-2 cells. *Nature* 316(6031):840-2.

30. Lennmyr F., Ericsson A., Gerwins P., Akterin S., Ahlstrom H., Terent A., (2004). Src family kinase-inhibitor PP2 reduces focal ischemic brain injury. *Acta Neurol Scand.* 110(3): 175-9.
31. Lewin S.L., Utley D.S., Cheng E.T., Verity A.N., Terris D.J., (1997). Simultaneous treatment with BDNF and CNTF after peripheral nerve transection and repair enhances rate of functional recovery compared with BDNF treatment alone. *Laryngoscope.* 107(7): 992-999.
32. Li Y.-S., Shyy J.Y.-J., Li S., Lee J., Su B., Karin M., Chien S., (1996). The Ras-JNK Pathway is Involved in Shear Induced Gene Expression. *Mol Cell Biol.* 16(11): 5947-54.
33. Lodish H., Berk A., Zipursky S.L., Matsudaira P., Baltimore D., Darnell, J., (2000). Molecular Cell Biology, Fourth Edition. New York, NY: W. H. Freeman and Company.
34. Luettich K., Schmidt C., (2003). TGFβ1 Activtes c-Jun and Erk 1 via αVβ6 Integrin. *Mol Cancer.* 2(1):33.
35. Maysinger D., Morinville A. (1997). Drug Delivery to the Nervous System. *Trends Biotechnol.* 15(10): 410-18.
36. O'Brien F.J., Harley B.A., Yannas I.V., Gibson L.J., (2004). Influence of freezing-rate on pore structure in freeze-dryed collagen-GAG scaffolds. *Biomaterials*, 25(6): 1077-86.
37. Okamoto-Inoue M, Taniguchi S, Sadano H, Kawano T, Kimura G, Gabbiani G, Baba T. (1990). Alteration in expression of smooth muscle alpha-actin associated with transformation of rat 3Y1 cells. *J Cell Sci.* 96 (Pt 4):631-7.
38. Pruss R.M., Herschman H.R., (1977). Variants of 3T3 Cells Lacking Mitogenic Response to Epidermal Growth Factor. *Proc. Natl Acad Sci. USA.* 74(9): 3918-21.
39. Racine-Samson L., Rockey D.C., Bissell D.M., (1997). The Role of α1β1 Integrin in Wound Contraction: A Quantitative Analysis of Liver Myofibroblasts In Vivo and in Primary Culture. *J Biol Chem.* 272 (49): 30911-17.
40. Ronnov-Jessen L., Petersen O.W., (1996). A Function for Filamentous alpha-Smooth Muscle Actin: Retardation of Motility in Fibroblasts. *J Cell Biol.* 134(1): 67-80.
41. Rufer M., Flanders K., Unsicker K., (1994). Presence and Regulation of Transforming Growth Factor Beta mRNA and Protein in the Normal and Lesioned Rat Sciatic Nerve. *J Neurosci Res.* 39(4): 412-23.
42. Scaffidi A.K., Moodley Y.P., Weichselbaum M., Thompson P.J., Knight D.A., (2001). Regulation of Human Lung Fibroblast Phenotype and Function by Vitronectin and Vitronectin Integrins. *J Cell Sci.* 114(Pt 19): 3507-16.
43. Schmidt C.E., Leach J. B. (2003). Neural Tissue Engineering: Strategies for Repair and Regeneration. *Annu. Rev. Biomed. Eng.* 5:293-347.
44. Sethi K., Yannas I.V., Mudera V., Eastwood M., McFarland C., Brown R.A., (2002). Evidence for Sequential Utilization of Fibronectin, Vitronectin, and Collagen During Fibroblast-Mediated Collagen Contraction. *Wound Rep Reg.* 10: 397-408.

45. Spilker M.H., Asano K., Yannas I.V., Spector M., (2001). Contraction of Collagen-Glycosaminoglycan Matrices by Peripheral Nerve Cells in Vitro. *Biomaterials* 22: 1085-1093.
46. Spilker M., Soog J., (2001). Unpublished data.
47. Tadashi I., Shigetomo F., Patel V., Katz B.Z., Yamada K.M., Gutkind J.S., (1999). Divergent Signaling Pathways Link Focal Adhesion Kinase to Mitogen-activated Protein Kinase Cascades. *J. Biol. Chem.* 274(43): 30738-46.
48. Thannickal V.J., Lee D.Y., White E.S., Cui Z., Larios J.M., Chacon R., Horowitz J.C., Day R.M., Thomas P.E., (2003). Myofibroblast Differentiation by Transforming Growth Factor β1 Is Dependent on Cell Adhesion and Integrin Signaling via Focal Adhesion Kinase. *J. Biol. Chem.* 278(14): 12384-9.
49. Todaro G.J., Green H., (1963). Quantitative Studies of the Growth of Mouse Embryo Cells in Culture and their Development into Established Lines. *J Cell Biol.* 17: 299-313.
50. Vaughan M. B., Howard E.W., Tomasek J.J., (2000). Transforming Growth Factor-β1 Promotes the Morphological and Functional Differentiation of the Myofibroblast. *Exp Cell Res.* 257(1): 180-9.
51. Vickers S.M., Johnson L.L., Zou L.Q., Yannas I.V., Gibson L.J., Spector M., (2004) Expression of alpha-smooth muscle actin by and contraction of cells derived from synovium. *Tissue Eng.*, 10(7-8): 1214-23.
52. Voet D., Voet J., (1995). Biochemistry, Second Edition. Somerset, NJ: John Wiley & Sons.
53. Yannas I.V., (2001). Tissue and Organ Regeneration in Adults. New York, NY: Springer-Verlag New York Inc.
54. Yannas I.V., Hill B.J., (2004). Selection of Biomaterials for Peripheral Nerve Regeneration Using Data from the Nerve Chamber Model. *Biomaterials* 25: 1593-1600.
55. Yoshizumi M. Abe J., Haendeler J., Huang Q., Berk B.C., (2000). Src and Cas Mediate JNK Activation but not Erk1/2 and p38 Kinases by Reactive Oxygen Species. *J. Biol. Chem.* 275(16): 11706-12.
56. Zaleskas JM, Kinner B, Freyman TM, Yannas IV, Gibson LJ, Spector M (2001). Growth factor regulation of smooth muscle actin expression and contraction of human articular chondrocytes and meniscal cells in a collagen-GAG matrix. *Exp Cell Res.* 270(1):21-31.